

A Survey of World Models for Autonomous Driving

Tuo Feng[✉], Wenguan Wang[✉], Senior Member, IEEE, Yang Yi[✉], Senior Member, IEEE

Abstract—Recent breakthroughs in autonomous driving have been propelled by advances in robust world modeling, fundamentally transforming how vehicles interpret dynamic scenes and execute safe decision-making. World models have emerged as a linchpin technology, offering high-fidelity representations of the driving environment that integrate multi-sensor data, semantic cues, and temporal dynamics. This paper systematically reviews recent advances in world models for autonomous driving, proposing a three-tiered taxonomy: (i) Generation of Future Physical World, covering Image-, BEV-, OG-, and PC-based generation methods that enhance scene evolution modeling through diffusion models and 4D occupancy forecasting; (ii) Behavior Planning for Intelligent Agents, combining rule-driven and learning-based paradigms with cost map optimization and reinforcement learning for trajectory generation in complex traffic conditions; (iii) Interaction between Prediction and Planning, achieving multi-agent collaborative decision-making through latent space diffusion and memory-augmented architectures. The study further analyzes training paradigms, including self-supervised learning, multimodal pretraining, and generative data augmentation, while evaluating world models' performance in scene understanding and motion prediction tasks. Future research must address key challenges in self-supervised representation learning, long-tail scenario generation, and multimodal fusion to advance the practical deployment of world models in complex urban environments. Overall, the comprehensive analysis provides a technical roadmap for harnessing the transformative potential of world models in advancing safe and reliable autonomous driving solutions.

Index Terms—Autonomous Driving, World Models, Self-Supervised Learning, Behavior Planning, Generative Approaches

1 INTRODUCTION

THE quest for autonomous driving is a focal point in both scientific research and industry endeavors. It aims to reduce traffic accidents, alleviate congestion, and enhance mobility for societal groups [1]. Current statistics underscore that human error remains the principal cause of accidents [2], indicating that reducing reliance on direct human control could lower the incidence of traffic-related fatalities and injuries. Beyond safety, economic factors also propel the development of autonomous driving technologies [3].

Despite these incentives, achieving high-level autonomy faces major hurdles. Foremost among these is perceiving and understanding dynamic traffic scenarios, which requires fusing heterogeneous sensor streams into an environmental representation [4], [5]. Autonomous vehicles must rapidly assimilate multi-modal data, detect salient objects, and anticipate their motion under adversarial conditions – such as sensor degradation in heavy rain, unpaved roads with poor markings, or aggressive traffic maneuvers [6], [7]. Moreover, real-time decision-making introduces computational constraints, imposing millisecond-level responsiveness to address unexpected obstacles or anomalous behaviors [8]. Equally pivotal is the system's resilience in extreme or long-tail scenarios (e.g., severe weather, construction zones, or erratic driving behaviors), where performance shortfalls can compromise overall safety [9], [10].

Within this context, constructing robust *world models* has emerged as a cornerstone. In essence, a world model is a generative spatio-temporal neural system that compresses multi-sensor physical observations into a compact latent state and rolls it forward under hypothetical actions, letting the vehicle rehearse futures before they occur [11], [12]. This high-fidelity internal map [3] updates online, and feeds downstream tasks such as physical-world prediction [13]. Recent work refines such models with generative sensor fusion [14]–[18], unifying heterogeneous inputs into consistent top-down views [19], [20].

These robust world models leverage environmental representations to optimize behavior planning, serving as a keystone for safer, efficient autonomous driving. By enabling trajectory optimization, real-time hazard detection, and adaptive route planning, they reduce predictable risks [5] and are compatible with vehicle-to-everything systems [8]. World models facilitate cohesive integration between perception and control subsystems, streamlining the closed-loop autonomy pipeline [21], [22].

Differences between Our Survey and Others. Existing surveys on world models for autonomous driving can be classified into two categories. The mainstream category covers general world models used across many fields [11], [23], with autonomous driving only one area. The second category [24], [25], though relatively scarce, focuses on the application of world models within autonomous driving. They categorize studies coarsely and often focus solely on world simulation or lack discussions on the interaction between planning and prediction, resulting in a lack of a clear taxonomy. In this paper, a comprehensive review of world models for autonomous driving is presented, and their applications are explored, thereby highlighting how these

• T. Feng, W. Wang and Y. Yang are with Collaborative Innovation Center of Artificial Intelligence (CCAI), Zhejiang University, China. (Email: fengtuo2015@outlook.com, wenguanwang.ai@gmail.com, yangics@zju.edu.cn)

• Corresponding Author: Wenguan Wang

• Paper List: <https://github.com/FengZicai/AwesomeWMAD>

• Benchmarks: <https://github.com/FengZicai/WMAD-Benchmarks>

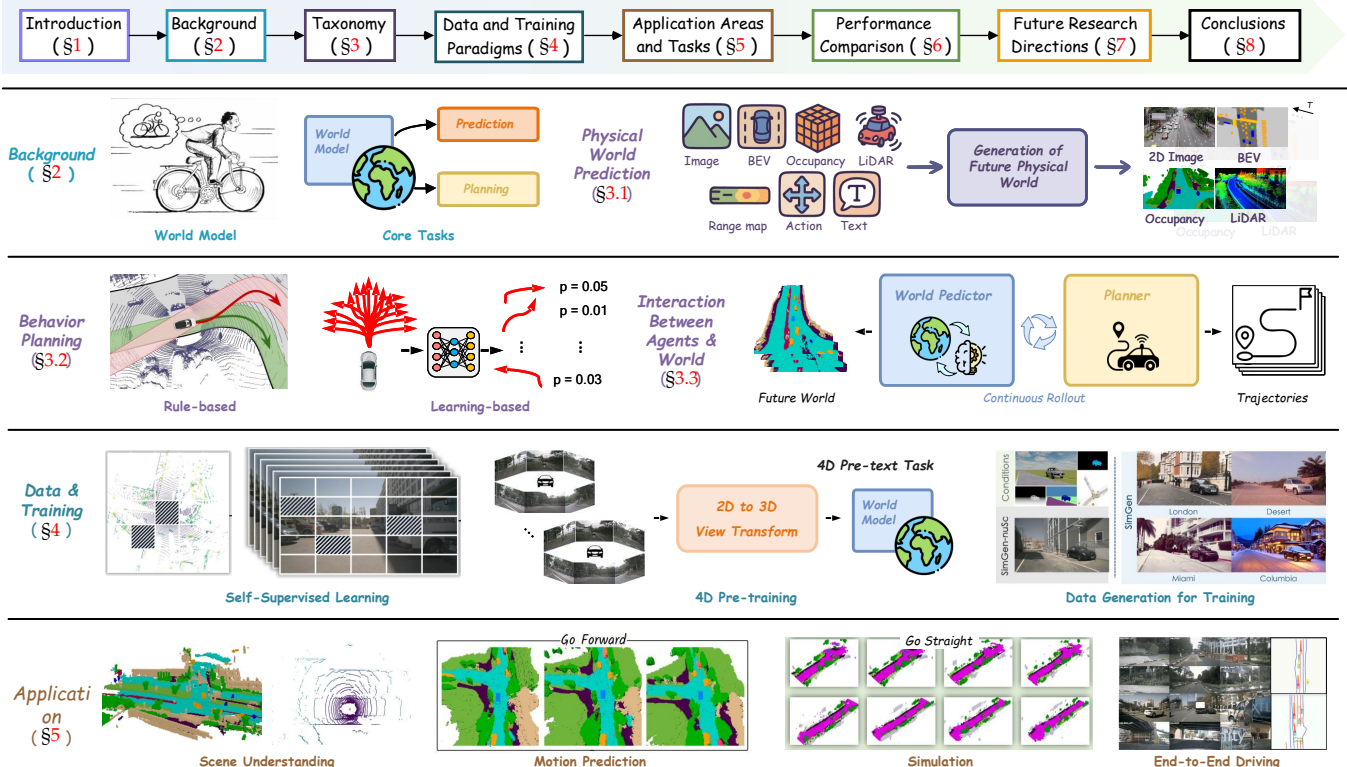


Fig. 1. **Structure of the overall review (§1).** The top row outlines the organization. The second and third rows illustrate the background and key components. The fourth row highlights various methodologies for training models in autonomous driving. The bottom row showcases four application areas for world models in autonomous driving.

models are shaped by and adapt to the automotive sector.

Goals of Our Survey. Guided by the principle that world models are central to the understanding of dynamic scenes, this survey aims to (i) develop a *comprehensive, structured taxonomy* of world models for autonomous driving highlighting the core architectures, input/output modalities, and conditioning strategies; (ii) classify the most commonly used datasets and evaluation metrics employed in world-model research for autonomous driving; and (iii) identify future research directions to advance the reliability and safety of world models in complex driving environments.

Current research falls into three key areas: (i) Generation of Future Physical World: Focusing on the physical world evolution of both dynamic objects and static entities [10], [18], [26]; (ii) Behavior Planning for Intelligent Agents: Examining generative and rule-based planning methods that produce safe, efficient paths under uncertain driving conditions [13], [27], [28]; (iii) Interaction between Behavior Planning and Future Prediction: Highlighting how unified frameworks can capture agent interactions and leverage predictive insights for collaborative optimization [29], [29]. Specifically, the following contributions are presented:

- ▶ **Analysis of Future Prediction Models:** Image-/BEV-/OG-/PC-based generation methods are examined to show how geometric and semantic fidelity is achieved, including 4D occupancy forecasting and diffusion-based generation.
- ▶ **Investigation of Behavior Planning:** Behavior planning is explored through both rule-based and learning-based approaches, and notable improvements in robustness and collision avoidance are demonstrated.
- ▶ **Proposition of Interactive Model Research:** Interactive

models that jointly address future prediction and agent behavior are reviewed, indicating how this synergy can enhance real-world adaptability and operational safety.

Four frontier challenges are highlighted – developing *self-supervised* world models, constructing *unified multi-modal* embeddings, building *advanced, physics-aware* simulators, and designing *lean, latency-aware* architectures – to chart a clear roadmap for next-generation autonomous driving research. As the research landscape expands and real-world adoption grows more urgent, this survey is intended to serve as a valuable reference for researchers and practitioners, laying the groundwork for safer, more robust autonomous-driving solutions.

A summary of this paper's structure is given in Fig. 1: §1 motivates world models for autonomous driving; §2 formalises the core tasks of world models; §3 introduces a taxonomy of existing methods; §4 contrasts prevailing data and training paradigms; §5 outlines key application areas; §6 benchmarks state-of-the-art models; §7 identifies open challenges and research opportunities; and §8 concludes the survey and summarizes key findings.

2 BACKGROUND

§2.1 first defines world models and their autonomous driving variant that fuses multi-modal inputs for long-horizon planning tasks; next, §2.2 states the formal problem, describing future-world generation and agent planning.

2.1 Definition of World Models

A world model is a generative spatio-temporal neural system that encodes the external physical environment into a

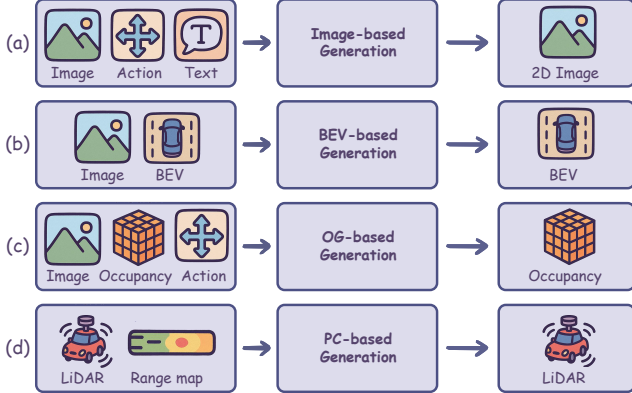


Fig. 2. **The paradigms of generation methods for future physical world** (§3.1). (a) Image-based generation synthesizes high-fidelity 2D images. (b) BEV-based generation forecasts BEV maps using paired image and BEV cues. (c) OG-based generation predicts 4D occupancy grids. (d) PC-based generation outputs future LiDAR sweeps. Boxes indicate processing modules; solid arrows denote data flow.

compact latent state, jointly capturing geometry, semantics and causal context [11]. This internal state is learned without labels: the system first employs a self-learning compressor to squeeze raw sensor frames into a handful of key numbers; next, a time-aware prediction module uses the hidden state and the agent’s action to infer what the next hidden state will be, allowing the agent to rehearse an entire trajectory in its “mind” before acting in the real world [12], [30]. Because every part of the pipeline is differentiable [12], the whole model functions as an interpretable virtual sandbox that supplies gradients, data samples, and “what-if” roll-outs, enabling the agent to make decisions more efficiently [11].

World Models for Autonomous Driving apply the same idea to road domains by mapping synchronized camera images, LiDAR sweeps, radar echoes and HD-maps into a single latent scene graph, thereby unifying perception and prediction within one representation [24]. Inside this latent space the model rolls forward the joint dynamics of surrounding traffic and the ego vehicle over long horizons [11], enabling realistic scene generation, multi-agent behaviour forecasting, trajectory evaluation and low-latency control – all while respecting the physical constraints and multimodal uncertainties endemic to real-world driving.

2.2 Core Tasks in World Models for Autonomous Driving

In autonomous driving, a critical aspect is accurately predicting the future states of both the ego vehicle and its surrounding environment. To address the core tasks, world models w in autonomous driving takes sensor inputs (including a set of multi-view images I and a set of LiDAR points P) collected from previous frames and infers the scene and trajectory for the next frames. Specifically, the ego trajectory at time $T+1$, denoted as τ^{T+1} , is predicted alongside the surrounding scene z^{T+1} . w models the coupled dynamics of the ego vehicle’s motion and the environment’s evolution. Formally, the function w is given by:

$$z^{T+1}, \tau^{T+1} = w((I^T, \dots, I^{T-t}), (P^T, \dots, P^{T-t})). \quad (1)$$

The first core task is generation of future physical world [20], [31]–[33], which involves forecasting the future

states of dynamic entities. This task emphasizes capturing potential interactions, stochastic behaviors, and uncertainties within rapidly changing and complex scenes. The second core task is behavior planning for intelligent agents [22], [27], [34], [35], focusing on generating optimal and feasible trajectories for the ego vehicle. It requires accounting for safety constraints, dynamic obstacles, traffic regulations, and real-time adaptability.

3 TAXONOMY

3.1 Generation of Future Physical World

Fig. 2 arranges future-scene generators into four tracks – image, Bird’s-Eye View (BEV), occupancy grid (OG) and point cloud (PC) – that jointly raise realism, from photoreal frames through map-level layouts to 4D voxels and LiDAR sweeps, all enabled by controllable diffusion and long-horizon forecasting.

3.1.1 Image-based Generation

Image-based future-prediction methods for autonomous driving use generative models to tackle limited data and dynamic environments. Synthesizing realistic images enlarges training data and strengthens perception and planning.

Dreamer Series. *Dreamer series* was first proposed for learning world models to address dynamic scene understanding in gaming and robotics [74]–[76], later expanded to autonomous driving with DriveDreamer [10]. It enables controllable video generation in high-density urban traffic using real-world driving data, though they remain limited to 2D outputs lacking spatial-temporal coherence. Subsequent research introduces DriveDreamer-2 [37], incorporating LLM-based prompting mechanisms to enhance interactivity and diversity. With further advancements, DriveDreamer4D [26] significantly extends model capabilities by utilizing world model priors to generate spatial-temporally coherent 4D driving videos, marking a transition from traditional 2D to advanced 4D video generation. ReconDreamer [39] explores online restoration techniques to achieve precise video reconstruction of dynamic scenes. WorldDreamer [40] expands the applicability of world models by pioneering masked token prediction for multi-modal generation, bridging text-to-video and action-to-video tasks, and moving towards general-purpose world model construction. The development of the *Dreamer series* demonstrates a clear trend: progressing from 2D to multi-dimensional video generation, transitioning from task-specific to general-purpose models, and shifting from closed, structured conditions toward more open and general natural-language-based conditions.

Diffusion-based Image Generation. The evolution of this type in autonomous driving are coalescing around two complementary thrusts: *controllable multi-view generation* (e.g., BEVControl [43] and DrivingDiffusion [14]), which use latent diffusion to render geometry-consistent videos from rich cues such as BEV layouts, text prompts and optical flow, and *high-fidelity spatio-temporal modelling*, where DriveWM [44] and Vista [46] push diffusion roll-outs to longer horizons and higher spatial resolutions, markedly boosting temporal coherence and per-frame detail. The field progresses through breakthroughs in *multi-modal conditions*: integrating ego trajectory, human-pose, and DINO appearance

TABLE 1
Overview of summary, methods and core architectures for Image-/BEV-based generation (§3.1.1 and §3.1.2).

Summary	Method	Pub.	Core Architecture	Input Modality & Control Condition	Output Modality	Training Dataset
<i>Image-based Generation</i>						
Dreamer Series	DriveDreamer [10]	ECCV'24	Diffusion Model	Text + Image + HDMap + Box + Actions	2D Image + Actions	nuScenes [36]
	DriveDreamer-2 [37]	AAAI'25	LLM + Diffusion Model	Text + HDMap + Box	2D Image	nuScenes [36]
	DriveDreamer4D [26]	CVPR'24	Diffusion Model + 4DGS	Text + Image + Trajectory	2D Image	Waymo [38]
	ReconDreamer [39]	CVPR'24	Diffusion Model	Image + HDMap + Box	2D Image	Waymo [38]
	WorldDreamer [40]	arXiv'24	LLM	Image + Video + Text + Action	2D Image	nuScenes [36]
	CarDreamer [41]	IOTI'24	World Model Backbone	Image + BEV + LiDAR + Radar	2D Image + Actions	CARLA [42]
Image-based Generation Diffusion Models	BEVControl [43]	arXiv'23	Diffusion Model	BEV + Image + Text	2D Image	nuScenes [36]
	DrivingDiffusion [14]	ECCV'24	Diffusion Model	Image + Layouts + Text + Optical Flow	2D Image	CARLA [42]
	Drive-WM [44]	CVPR'24	Diffusion Model	Image + Action + Box + Map + Text	2D Image	nuScenes [36] + Waymo [38]
	DriVerse [45]	CVPR'25	Diffusion Model	Image + Trajectory	2D Image	nuScenes [36] + Waymo [38]
	GEM [16]	CVPR'24	Diffusion Model	Image + Trajectory + Human pose + DINO features	2D Image + Depth	Self-created dataset [16]
	Vista [46]	NeurIPS'24	Diffusion Model	Image + Action	2D Image	Self-created dataset [46]
	SimGen [47]	NeurIPS'24	Diffusion Model	Image + Depth + Segmentation + Text	2D Image	DIVA [47] + nuScenes [36]
	Delphi [48]	arXiv'24	Diffusion Model	Image + BEV layout + Failure Case	2D Image	nuScenes [36]
	BevWorld [32]	arXiv'24	Diffusion Model	Image + Point cloud + Action	2D Image + 3D LiDAR	nuScenes [36] + CARLA [49]
	DrivePhysica [50]	arXiv'24	Diffusion Model	Image + Poses + Box + Lane + Text	2D Image	nuScenes [36]
	Image-2-Drive [51]	arXiv'24	Diffusion Model	Image	2D Image	CARLA [49]
	MaskGWM [52]	arXiv'25	Diffusion Model	Image + Text + Action	2D Image	OpenDV-2K [53] + nuScenes [36]
	EOTWM [54]	arXiv'25	Diffusion Model	Image + Text + Trajectory	2D Image	nuScenes [36]
	UniFuture [55]	arXiv'25	Diffusion Model	Image + Depth	2D Image + Depth	nuScenes [36]
Image-based Generation Transformers	DiVE [56]	arXiv'25	Diffusion Model	Image + Text + Box + Road condition	2D Image	nuScenes [36]
	CoGen [57]	arXiv'25	Diffusion Model	Image + Occupancy	2D Image	nuScenes [36]
	GAIA-2 [58]	arXiv'25	Diffusion Model	Image + Action + Text	2D Image	Internal dataset [58]
	MiLA [59]	arXiv'25	Diffusion Model	Image + Waypoints + Text + Camera parameters	2D Image	nuScenes [36]
	DiST-4D [60]	arXiv'25	Diffusion Model	Image + Trajectory + BEV + Pose + Box	RGBD image	nuScenes [36] + Waymo [38]
	GAIA-1 [15]	arXiv'23	Transformer	Image + Action + Text	2D Image	Internal dataset [15]
	HoloDrive [61]	arXiv'24	Transformer	Image + LiDAR + Layouts + Text	2D Image + 3D LiDAR	nuScenes [36]
	BEVGen [62]	RA-L'24	Transformer	Image + BEV layout	2D Image	nuScenes [36] + Argoverse 2 [63]
Image-based Generation Transformers	DrivingWorld [64]	arXiv'24	Video GPT	Image + Orientation + Location	2D Image	NuPlan [65] Internal data [64]
	DriveSim [66]	arXiv'24	MLLMs	Image + Text	2D Image	Internal dataset [66]
	TMPE [35]	arXiv'24	Transformer	Image + Path + Speed	2D Image + BEV	CARLA [42]
	NeMo [67]	ECCV'24	Transformer	Image	2D Image + LiDAR + Occupancy	nuScenes [36]
	FUTURIS [68]	arXiv'25	Transformer	Segmentation + Depth	Segmentation + Depth	Cityscapes [69]
	<i>BEV-based Generation</i>					
BEV-based Generation	FIERY [33]	ICCV'21	Transformer	Image + Ego motion	BEV	nuScenes [36]
	StretchBEV [70]	ECCV'22	LSTM	Image	BEV	nuScenes [36]
	MILE [34]	NeurIPS'22	RNN	Image + BEV segmentation + Action	Image + BEV + Action	CARLA [49]
	UNO [31]	CVPR'24	CNN	LiDAR	Occupancy + LiDAR + BEV	nuScenes [36]
	PowerBEV [71]	IJCAI'23	CNN	Image	BEV Instance	nuScenes [36]
	GenAD [22]	ECCV'24	Transformer	Image + BEV	Map + Trajectory	nuScenes [36]
	CarFormer [72]	ECCV'24	Transformer	BEV + Trajectory + Destination + Traffic sign	BEV + Action	Longest6 [73]

tokens for behaviour-aware video synthesis [16]; translating simulator layouts into photorealistic scenes through a cascade diffusion pipeline [47] or dual-scale controlNet-stable diffusion [77]; uniting LiDAR and camera streams in a BEV latent grid for geometry-consistent cross-sensor forecasting [32]; aligning ego-other vehicle trajectories in latent space to enable fully controllable, multi-agent video generation [54]; and grounding multi-camera driving video generation in physics by aligning ego-world coordinates, injecting 3D flows, and box-guided occlusion reasoning [50]. Recent methods [45], [48], [55]–[59] focus on expanding from simple RGB image generation to more *diverse and enriched paradigms*, including extending conventional RGB prediction to jointly generate both images and depth [55]; shifting from layout-conditioned synthesis to fine-grained trajectory-conditioned control [45]; moving beyond 2D-only conditioning toward multi-view consistent generation [56]; transitioning from 2D layout cues to full 3D scene conditioned synthesis [57]; broadening single-view synthesis into multi-view, multi-agent interactive scenarios [58]; progressing from short-term clips to long-horizon video generation [59]; and further leveraging failure-case augmentation for robustness [48]. This technical evolution reveals a clear trend from isolated scene generation to integrated closed-loop simulation systems, providing high-fidelity, scalable synthetic environments for autonomous driving.

Transformer-based Image Generation. Transformer-based driving imagers are evolving from *narrow, single-view renderers* into *holistic, action-aware world models*. Cross-view architectures such as HoloDrive [61] and BEVGen [62] fuse camera and LiDAR or lift BEV layouts to street-level frames, unifying 2D appearance with 3D geometry. A *parallel line scales* sequence modeling: DrivingWorld [64] and GAIA-

[15] treat video, text and control as one token stream, enabling minute-long, controllable clips with coherent semantics. These token factories prove that unsupervised prediction alone can encode road rules and actor intent. *Complementary work* probes limits and remedies: DriveSim [66] exposes causal hallucinations in multimodal LLMs, while a DINOv2-based multi-view encoder [35] compresses synchronized front views into a latent scene grid that decodes to both RGB and BEV semantics, reducing covariate shift.

Summary. Table 1 shows different modern image-centric generative frameworks, which use diffusion and transformer architectures to produce diverse driving data. Several observations can be drawn:

- These methods synthesize photorealistic images to enrich training sets. They also create rare or safety-critical scenarios that are hard to capture in real data.
- World models forecast future states conditioned on actions. Fusion of multiple modalities enhances planning and dynamic reasoning.

3.1.2 BEV-based Generation

BEV Representation. A BEV representation unifies multi-modal sensor streams into a single top-down map, exposing lane layouts, dynamic actors, and free space in a planner-friendly format [32]. By stripping away perspective distortions, BEV methods provide high-level, spatially coherent context that has become a powerful complement – or even alternative – to image-centric pipelines, supporting tasks such as motion prediction and long-horizon trajectory forecasting. This 2D projection, however, gains simplicity at the expense of depth resolution: BEV maps can struggle

to retain fine-grained 3D geometry in scenes with complex vertical structure or steep depth gradients [78].

Starting with the probabilistic BEV forecaster FIERY [33], researchers stretch temporal range with StretchBEV [70], learn continuous 4D occupancy fields with UnO [31], and cut computation via the 2DCNN design [71]. *Object-centric* slots then emerge: CarFormer [72] assigns every actor a latent slot. MILE [34] compresses the whole scene into a single compact latent with the driving policy, enabling *policy-aware, multi-modal* prediction. Together, these advances unlock *generative planning*; GenAD [22] rolls the latent forward to sample ego-conditioned futures, BEVControl [43] lets users overwrite it with editable sketches for safety auditing, and ViDAR [20], although operating in point-cloud space, supplies geometry-aware pre-training that lifts BEV performance across the board. Together these works chart a path from early probabilistic forecasts to *efficient, object-aware, user-controllable* world models.

Summary. Table 1 summarizes recent BEV-based generative methods, which predict future BEV representations for autonomous driving tasks. Several observations can be drawn:

- ▶ Early works transform monocular images into probabilistic BEV maps, whereas newer models incorporate object-centric slots, 4D occupancy fields, and trajectory-conditioned latents to capture richer semantics and multi-agent interactions.
- ▶ Recent approaches move beyond supervised training by adopting self-supervised occupancy learning, lightweight multi-scale designs, and editable BEV sketches, paving the way toward closed-loop, generative world-model simulation.

3.1.3 OG-based Generation

OG Representation. An OG representation divides the driving scene into 3D voxels and assigns each cell a probability of being occupied, producing a single lattice that simultaneously tracks static structure and moving actors. This discretisation yields far richer geometric detail than 2D projections such as BEV, enabling fine-grained reasoning about scene evolution and actor interactions – qualities that have made OGs a mainstay of future-state prediction in autonomous driving. The price of this fidelity, however, is steep: dense voxel grids demand considerable memory and computational throughput, which can hinder deployment in large-scale or real-time systems [83].

OG-based Generation (*i.e.*, occupancy forecasting) originates from forecasting semantic occupancy grids on BEV [28], [113]–[117]. It is employed to predict how the surrounding occupancy will evolve in the near future.

CNN-based OG Generation. Occ4cast starts this type by unifying sparse-to-dense completion and 4D forecasting into a coherent Eulerian grid that reconstructs geometry and predicts its future [79]. Cam4DOcc then ports this paradigm from LiDAR to low-cost multi-view cameras, releasing a benchmark and network that align per-view geometry with motion cues [80]. Finally, PreWorld trims supervision demands by introducing a semi-supervised, two-stage pipeline that distills 2D imagery into 3D occupancy and planning priors [82]. These milestones trace a clear trajec-

tory: from dense LiDAR-based geometry, through camera-centric low-cost sensing, to label-efficient world models.

Transformer-based OG Generation. Many recent leading methods of this type adopt Transformer-based core architectures. These models act as vision-centric world models for autonomous driving and are designed to learn from pre-collected, open-loop benchmarks; hence they sit outside “Interaction between Planning and Prediction”.

Transformer-based OG research starts with MUVO [84], which fuses camera + LiDAR features in a voxel-level Transformer to predict 3D occupancy, yet its deterministic rollout and label hunger limit scalability. OccWorld [85] converts these voxels into autoregressive scene tokens, while DFIT-OccWorld [86] decouples dynamic-static warping to cut training cost, collectively launching a generative, token-based line of work. Toward perception-control unity, Drive-World [21] pre-trains a memory-augmented world model for downstream planning, and Drive-OccWorld [88] adds trajectory-conditioned heads so the same tokens directly score driving costs. *Efficiency* remains a parallel thread – OccProphet [92] refines compute, and T³Former [94] sparsifies temporal attention with triplane features, achieving real-time, camera-only deployment. OccLLAMA [89] and Occ-LLM [93] broaden the token vocabulary to *language and action*, enabling instruction-driven occupancy reasoning across the same generative backbone. Collectively, the field has evolved from deterministic voxel Transformers through autoregressive token worlds and efficiency-focused triplane models to *multimodal, instruction-aware, real-time world models*. Some studies attempt to introduce *3D Gaussian Splatting* (3DGS) into this field. GaussianWorld [90] treats occupancy as a 4D forecasting task in Gaussian space, explicitly factorising ego motion, local dynamics and scene completion; RenderWorld [91] removes all lidar by pairing a self-supervised Img2Occ labeler with an AM-VAE encoder and the same autoregressive backbone, yielding a compact, vision-only pipeline. Overall, these studies trace a path from heavy deterministic voxel fusion to lightweight stochastic tokenised representations, from perception-only forecasting to memory- and planning-conditioned roll-outs, and from single-modality grids to language-grounded multi-sensor inputs; the overall trend converges on *controllable, efficient, multi-modal* world models.

Diffusion-based OG Generation. Diffusion-based OG generation methods enable fine-grained control by coupling spatio-temporal diffusion transformers with compact 4D tokens. They further advance toward *controllable, token-efficient, multi-modal* world models by: introducing trajectory-resampling control to steer future occupancy synthesis [95]; compressing scenes into compact 4D tokens for coherent occupancy videos [18]; projecting 4D voxels onto HexPlanes and rolling them out with DiT for large-scale semantic forecasting [17]; and diffusing unified BEV semantic grids into joint video + LiDAR streams [96].

Summary. Table 2 assembles recent OG generative frameworks using CNNs, Transformers, and diffusion models for 4D occupancy forecasting. Several observations emerge:

- ▶ The field migrates from heavy, deterministic voxel fusion to lightweight, stochastic tokenisation and further to Gaussian splats, reducing memory cost.

TABLE 2
Overview of summary, methods and core architectures for OG-/PC-based generation (§3.1.3 and §3.1.4).

Summary	Method	Pub.	Core Architecture	Input Modality & Control Condition	Output Modality	Training Dataset
<i>OG-based Generation</i>						
OG-based Generation CNNs	Occ4cast [79]	IROS'24	CNNs	LiDAR	Occupancy	OCFBench [79]
	Cam4DCC [80]	CVPR'24	CNN	Image + Ego motion + GMO + GSO	Occupancy	OpenOccupancy [81]
	PreWorld [82]	ICLR'25	CNN	Image + Occupancy	Occupancy	Occ3D [83]
OG-based Generation Transformers	MUVO [84]	IV'23	Transformer	Image + LiDAR + Action	Image + LiDAR + Occupancy	CARLA [42]
	OccWorld [85]	ECCV'24	Transformer	Occupancy + Trajectory	Occupancy + Trajectory	Occ3D [83]
	DFIT-OccWorld [86]	arXiv'24	Transformer	Occupancy + Image + Ego poses	Occupancy + Image + Trajectory	Occ3D [83] + OpenScene [87]
	DriveWorld [21]	CVPR'24	Transformer	Image + Action	Occupancy + Action	nuScenes [36] + OpenScene [87]
	Drive-OccWorld [88]	AAAI'25	Transformer	Image + Action	Occupancy + Flow + Trajectory	nuScenes [36] + OpenOccupancy [81]
	OccLLaMA [89]	arXiv'24	Transformer	Occupancy + Trajectory + Text	Occupancy + Trajectory + Text	nuScenes [36] + OpenOccupancy [81]
	GaussianWorld [90]	CVPR'25	Transformer + 3DGs	Gaussians + Image	Occupancy	nuScenes [36]
	RenderWorld [91]	ICRA'24	Transformer + 3DGs	Image	Occupancy + Trajectory	nuScenes [36]
	OccProphet [92]	ICLR'25	Transformer	Image	Occupancy + Flow	nuScenes [36] + OpenOccupancy [81]
OG-based Generation Diffusion Models	Occ-LLM [93]	ICRA'25	LLM	Image + Occupancy	Occupancy + Trajectory + Text	nuScenes [36] + Occ3D [83]
	T ³ Former [94]	arXiv'25	Transformer	Occupancy	Occupancy + Trajectory	nuScenes [36]
	DOME [95]	arXiv'24	Diffusion Model	Occupancy + Action	Occupancy	nuScenes [36]
	OccSora [18]	arXiv'24	Diffusion Model	Occupancy + Trajectory	Occupancy	Occ3D [83]
OG-based Generation Diffusion Models	UniScene [96]	arXiv'24	Diffusion Model	BEV Layouts + Text	Occupancy + LiDAR + Image	OpenOccupancy [81] + nuScenes [36]
	DynamicCity [17]	ICLR'25	Diffusion Model	Occupancy + Command + Trajectory + Layout	Occupancy	Occ3D [83] + CarlaSC [97]
<i>PC-based Generation</i>						
PC-based Generation CNNs	PCP [98]	CoRL'22	CNN	LiDAR + Range map	LiDAR	KITTI [99]
	4DOcc [100]	CVPR'23	CNN	LiDAR	Occupancy + LiDAR	KITTI [99] + nuScenes [36]
PC-based Generation Transformers	PCPNet [101]	RA-L'23	CNN	LiDAR + Range map	LiDAR	KITTI [99]
	ViDAR [20]	CVPR'24	Transformer	Image + Action	LiDAR	nuScenes [36]
	HERMES [102]	arXiv'25	Transformer	Image + Text + Action	LiDAR + Text	nuScenes [36]
PC-based Generation Diffusion Models	LiDARGen [103]	ECCV'22	Diffusion Model	LiDAR + Range map	LiDAR	KITTI-360 [104]
	Copilot4D [105]	ICLR'24	Diffusion Model	LiDAR	LiDAR	KITTI [99] + nuScenes [36]
	RangeLDM [106]	arXiv'24	Diffusion Model	LiDAR + Range map	LiDAR	KITTI-360 [104]
PC-based Generation Others	Lidarsim [7]	CVPR'20	Composition	LiDAR	LiDAR	Internal dataset [7]
	lidarGeneration [107]	IROS'19	VAE + GAN	LiDAR + Point map	LiDAR	KITTI [99]
	UltraLiDAR [108]	CVPR'23	VQ-VAE	LiDAR	LiDAR	KITTI-360 [104] + nuScenes [36]
	SPFNet [109]	CoRL'21	LSTMs	LiDAR + Range map	LiDAR	KITTI [99] + nuScenes [36]
	S2net [110]	ECCV'22	LSTMs	LiDAR + Range map	LiDAR	KITTI [99] + nuScenes [36]
	NFL [111]	ICCV'23	Nerf	LiDAR	LiDAR	KITTI [99]
	Nerf-lidar [112]	AAAI'24	Nerf	LiDAR + Image + Segmentation	LiDAR	nuScenes [36]

- Occupancy world models evolve beyond perception-only roll-outs: memory-augmented and trajectory-conditioned heads embed planning cues, and language-grounded tokens enable instruction-driven reasoning.
- Efficiency and controllability become central themes: dynamic/static warping, sparse triplane attention, and diffusion-based controllable priors. This pushes OG generation toward real-time, scalable simulation.

3.1.4 PC-based Generation

PC Representation. A PC representation encodes the world as the raw 3D points returned by LiDAR, preserving fine-grained 3D details for vehicles, pedestrians, and surrounding infrastructure. This fine spatial fidelity makes PCs indispensable for occupancy forecasting, dynamic-scene modelling, and predictive reconstruction in autonomous driving. However, the sparsity and irregular sampling of LiDAR scans – combined with real-time computational constraints – continue to pose significant algorithmic challenges. In response, LiDAR point cloud generation, a subtask of 3D point cloud generation, has gained increasing attention to address these limitations and enhance downstream perception and planning capabilities.

Similar to OG-based generation, PC-based generation predicts future 3D point clouds from past LiDAR sweeps.

CNN-based PC Generation. PCP [98] stacks consecutive range images into a 3D spatio-temporal volume and applies 3D CNNs that fuse geometry with motion cues for consistent temporal modelling. 4DOcc [100] discretizes historical scans into 4D occupancy grids and leverages lightweight CNN temporal modules to forecast future occupancy, lowering annotation demands while preserving scene fidelity.

Transformer-based PC Generation. PCPNet [101] enriches range-image sequences by inserting self-attention layers that capture long-range dependencies, producing temporally consistent point clouds with stronger context

ual cues. ViDAR [20] frames vision-LiDAR pre-training as an autoregressive task: it embeds images and actions with a Transformer encoder and decodes future point sequences causally, providing geometry-aware priors that benefit downstream BEV generation. Building on this, HERMES [102] fuses multi-view images and textual prompts into BEV embeddings through causal attention, then employs differentiable voxel rendering, constrained by motion and collision losses, to synthesize high-fidelity point clouds that respect scene dynamics.

Diffusion-based PC Generation. LiDARGen [103] formulates LiDAR synthesis as a score-matching diffusion process on equirectangular range images, producing physically plausible and controllable samples. Copilot4D [105] discretizes LiDAR observations with a VQ-VAE and conducts discrete diffusion to autoregressively sample future sweeps, enabling unsupervised world-model learning. RangeLDM [106] denoises latent representations of range-view images to reconstruct accurate point clouds, combining latent diffusion with Hough-voting projections.

Other PC Generation Methods. Early GAN-based frameworks [118] support unconditional point-cloud synthesis, while lidarGeneration [107] specifically mimics real-world LiDAR statistics via adversarial training on range-image projections. SPFNet [109] and S2net [110] employ LSTMs on sequential range maps with explicit compensation for sensor calibration. Lidarsim [7] couples physical raycasting with learned noise models to generate near-realistic scenes. UltraLiDAR [108] uses discrete latent tokens to preserve structural and semantic consistency. Neural-field methods (*i.e.*, NFL [111] and Nerf-LiDAR [112]) extend NeRF paradigms to LiDAR, enabling novel-view synthesis under dynamic and partially observed conditions.

Summary. Table 2 shows different modern LiDAR generation frameworks. Several observations can be drawn:

- PC-based Generation leverages diverse architectures (*e.g.*,

TABLE 3
Overview of representative learning-based planners (§3.2.1).

Summary	Method	Pub.	Core Architecture	Input Modality & Control Cond.	Output Modality	Training Dataset
<i>RL & MPC planners</i>						
Model-free RL	PFBD [13]	Electronics'19	TD3 policy net	Gap + Speed + Curvature	Manoeuvre cmd.	Internal [13]
Deterministic Ensemble	MILE [34]	NIIPS'22	Latent dynamics + MPC	Image sequence + ego state	Trajectory	CARLA expert logs [42]
Uncertainty-aware	AdaptiveDrive [119]	ICRA'24	BehaviorNet + MPC	Agent histories + HD-map	Trajectory	nuPlan [65]
	UMBRELLA [120]	RA-L23	Ensemble + Unc. propag.	Vehicle state history	Trajectory	NGSIM [121] + CARLA [122]
	AdaWM [123]	ICLR'25	Low-rank adaptive WM	State + reward	Trajectory	nuPlan [65]
Agent-centric/Analytic	CarDreamer [41]	IoT'24	Actor-wise latent intents	Tracks + map	Multi-agent traj.	CARLA [42]
	Dream2Drive [124]	arXiv'25	Diff. physics WM	State + goal	Trajectory	WOMD [125]
Latent accelerator	Think2Drive [126]	ECCV'25	Latent-space planner	Latent WM	Trajectory	CARLA-V2 [122]
<i>LLM-based planners</i>						
Autoreg. Transformer	DrivingGPT [127]	arXiv'24	MM GPT-style decoder	Image + ego state	Action tokens	nuPlan [65]
	VaViM [128]	arXiv'25	Video-Gen. Transformer	Video + ego	Action tokens	OpenDV [53] & nuPlan [65] & nuScenes [36]
BEV scorer	WoTE [129]	arXiv'25	BEV head + sampler	BEV grid + cand. traj.	Score vector	nuScenes [36]
Sparse-token WM	SSR [130]	ICLR'25	Sparse token WM	BEV features	Action tokens	nuPlan [65]
Vision-LLM sim.	DriveSim [66]	arXiv'24	GPT-4V probe	Lang. cmd. + frames	Sim. trajectory	Internal [66]
<i>Volume-based planners</i>						
Volume-based	DSDNet [131]	ECCV'20	CNN cost-volume	Image + BEV map	Trajectory set	nuScenes [36]
Hybrid Cost Volume	ST-P3 [27]	ECCV'22	Spatio-temp. CNN	Image seq.	Trajectory set	nuScenes [36]
	MP3 [28]	CVPR'21	Unified map-predict-plan	Multi-modal	Trajectory set	nuScenes [36]
	NEAT [132]	ICCV'21	Attention fields	Image + HD-map	Trajectory set	nuScenes [36]
	NMP [133]	CVPR'19	Neural motion planner	LiDAR + HD-map	Trajectory set	Internal [133]
	PPP [115]	ECCV'20	Semantic BEV planner	BEV semantics	Trajectory set	nuScenes [36]
Occupancy volume	Occ-WM [88]	AAAI'25	4D occ. WM + Q-net	4D occupancy	Trajectory	nuScenes [36] + Occ3D [83]

Diffusion Models, GANs, VQ-VAE, and NeRF) to address LiDAR sparsity and irregularity while preserving geometric fidelity. Methods like LiDARGen and UltraLiDAR explicitly model physical sensor constraints, whereas Nerf-LiDAR and NFL integrate neural rendering to enhance novel-view synthesis under dynamic scenarios.

- Recent advancements prioritize integrating world models and multi-modal inputs. However, most approaches focus on geometric priors of LiDAR data, with limited exploration of semantic-aware generation or perceptual consistency for downstream tasks.

3.2 Behavior Planning for Intelligent Agents

Behavior planning translates a rich, ever-changing scene understanding into a safe, comfortable, goal-directed trajectory. Most methods first sample diverse, kinematically feasible motions and then, guided by semantic predictions and tactical cues, select the most likely candidate [28], [131], [134]. This likelihood-based scoring fuses predicted dynamics, traffic rules, and comfort metrics, yielding a path that adapts smoothly to evolving conditions while meeting stringent safety requirements.

3.2.1 Learning-based Planning

Early autonomous-vehicle planners relied on rule-based heuristics, but these brittle hand-crafted pipelines struggle with the combinatorial variety of urban traffic and become hard to maintain as the rule set expands [135]–[137]. Learning-based motion planning gained traction once large-scale driving logs and fast GPUs became available [6]. Modern architectures ingest multimodal sensor streams (*i.e.*, LiDAR, RADAR, GPS signals [138] and camera frames [139], [140]) to output lane-change choices [141], [142], future state distributions [143], reference paths [144], or direct control commands such as steering and throttle [145]–[147].

Offline supervision or reinforcement learning allows these networks to keep online inference fast and to adapt to new scenes when supplied with sufficient diverse data. Compared with rule-based planning, data-driven planners handle uncertainty and interaction richness more gracefully, especially when reinforced by graph neural networks, attention mechanisms, or large language models that encode

high-level traffic intent [148]–[150]. However, three open issues remain: (i) generalisation: performance still degrades in out-of-distribution weather, geography, or traffic densities; (ii) interpretability: opaque latent policies impede validation and debugging [145], [147], [151]; and (iii) formal safety guarantees: current learning pipelines lack provable bounds required for certification [152]. Addressing these gaps is central to scaling learning-based behavior planning from research prototypes to trustworthy real-world deployment.

RL & MPC Planners. *Model-free reinforcement-learning (RL)* planner [13] employs a twin-delayed deep deterministic policy gradient (TD3) that maps high-level planning features to manoeuvre commands, delegating the final continuous trajectory to a downstream generator. *Model-based RL* planners span a spectrum of world-model granularity and safety mechanisms. Early deterministic offline ensembles [34] learn compact latent dynamics and couple them with Model Predictive Control (MPC) to deliver fast, sample-efficient roll-outs and transparent constraint handling, yet they over-commit when aleatoric noise appears in multi-agent traffic. Building on this paradigm, the follow-up work [119] performs planning with adaptive world models, learning a closed-loop social world model and embedding it within MPC – an explicit instantiation of model-based RL tailored to urban traffic. *Uncertainty-aware* variants [120], [123] inject stochastic ensembles or adaptive low-rank updates, exposing epistemic and aleatoric risk for more robust out-of-distribution reasoning, though at the price of heavier sampling and fine-tuning overheads. *Agent-centric and analytic* approaches [41], [124] model each actor separately – using attention-based latent intents or differentiable physics – to capture nuanced social interactions, but they rely on accurate tracks or hand-coded dynamics. *Latent-space* accelerators [126] plan entirely in a low-dimensional latent, enabling orders-of-magnitude faster roll-outs on modest hardware, yet abstract states can omit critical geometry such as traffic-light phase and undermine fine manoeuvres.

LLM-based Planners. *Autoregressive multimodal transformers* [127], [128] treat driving as next-token prediction over interleaved image-and-action tokens, coupling perception, world modelling and control, and achieving strong nuPlan and NAVSIM results, but they demand high-end multi-GPU compute and still struggle with long-horizon consistency and safety certification. WoTE adds a lightweight bird's-eye-

view predictor that scores sampled trajectories online, boosting safety with minimal latency, yet its fidelity is capped by BEV grid resolution and the quality of the trajectory sampler [129]. SSR compresses dense BEV features into just 16 navigation-guided tokens, cutting FLOPs while maintaining accuracy, though aggressive sparsification risks missing rare but critical actors or occlusions [130]. DriveSim explores *GPT-4V-style* models as internal simulators for language-conditioned planning, showing promising affordance reasoning but revealing frame-order errors and inconsistent imagined trajectories that limit closed-loop reliability [66].

Volume-based Planners. Hybrid *cost-volume* methods first sample or generate a diverse set of candidate trajectories and then rank them with a composite cost that fuses hand-crafted comfort or rule-compliance terms with likelihoods predicted from learned occupancy or segmentation maps. To preserve interpretability, such planners explicitly build a cost map, pair it with a trajectory sampler, and execute the candidate with the lowest overall cost. Concretely, *cost-volume* planners [28], [115], [133], [153] compute a confidence score for each sampled trajectory from the cost volume, guiding the choice toward paths that best balance safety, efficiency, and rule compliance. This approach yields interpretable, safety-oriented plans, but its effectiveness diminishes when the sampler cannot cover the dense combinatorial space of urban traffic [27], [28], [115], [131]–[133]. By contrast, *occupancy volume* method replaces heuristic costs with a learnable head applied to 4D occupancy forecasts, providing richer collision cues and enabling end-to-end fine-tuning, albeit at the expense of higher memory footprints and a reliance on dense occupancy supervision [88].

Summary. Table 3 shows compares major learning-based planning paradigms. Several observations can be drawn:

- ▶ Modern planners fuse LiDAR, RADAR, GPS and vision, sample kinematic motions, and rank them with learned semantic, interaction, and rule cues, yielding adaptable trajectories beyond brittle heuristics.
- ▶ Architectures diverge: RL and MPC planners fuse latent dynamics, uncertainty, safety; LLM transformers cast driving as token prediction; cost-volume planners rank sampled paths via learned occupancy costs.
- ▶ Gaps remain: models falter in novel weather, policies stay opaque, safety proofs are lacking, and heavy compute blocks real-time urban use, urging work on robust, interpretable, certifiable planners.

3.2.2 Rule-based Planning

Rule-based planners endure because they guarantee safety and are easy to audit [171], [172]. They treat motion as a deterministic optimisation over explicit dynamics and hand-crafted costs, yielding transparent behaviour. Four core families dominate: car-following laws (e.g., IDM), sampling planners (RRT, state lattice), model-predictive control, and potential-field navigation. Modern stacks combine these blocks for interpretability and safety, yet modular fusion can lose global optimality and fixed heuristics struggle in dense, fast-changing traffic.

Car-following Models. Physics-inspired longitudinal models translate the instantaneous gap, speed and closing rate into throttle or brake commands. The Intelligent Driver

Model and its calibrated siblings capture free-flow, synchronized and stop-and-go regimes with a single continuous formula [154]. Recent work samples multiple IDM roll-outs and selects the minimum-cost, safety-compliant candidate to improve comfort without losing closed-form guarantees [155]. Because these laws are purely algebraic, production-grade Adaptive Cruise Control (ACC) systems can execute them at tens-to-hundreds Hz frequencies. However, their inherently short prediction horizon is a key limitation, so modern planners augment analytic commands with map priors or predictive MPC to anticipate intersections and cut-in maneuvers better.

Sampling-based Planners. Sampling-based planners probe the vehicle’s configuration space with a sequence of samples, accept only collision-free continuations, and then rank feasible motion sequences with handcrafted costs. They split into two sub-families that trade optimality for speed in different ways. *Random sampling* methods grow a tree or roadmap toward stochastically chosen states, guaranteeing probabilistic completeness and – when augmented with rewiring – asymptotic optimality. Classic Rapidly-Exploring Random Trees (RRT) [156], [157] realise millisecond-level feasibility checks for single-query problems. Their optimal variants, RRT and RRG, refine paths online by incremental rewiring [158], [159]. Closed-loop extensions embed vehicle dynamics for high-speed manoeuvres, as demonstrated on MIT’s “Talos” car in the DARPA Urban Challenge [173], [174] and in multi-agent settings [175]. *Deterministic sampling* methods pre-tile the state–time space with kinematically feasible motion primitives, then apply graph search to pick the lowest-cost, collision-free sequence. Spatiotemporal lattices and their conformal highway variant capture curvature and speed limits explicitly [160], [161]. Polynomial libraries (cubic, quintic, B-spline) further reduce runtime by storing analytically smooth segments that satisfy dynamic bounds [176], [177]. Discretised terminal manifolds shrink search depth for time-critical street scenarios [162], and the Stanford “Junior” entry shows how such libraries integrate into a full urban-driving stack [178]. Because the candidate set is finite, deterministic planners sacrifice global optimality for predictable timing, making them popular for production autonomous vehicle stacks.

Continuous Optimisation. Continuous optimisation planners rebuild vehicle paths in continuous space each control cycle, casting curvature and speed as variables in a quadratic or nonlinear program constrained by dynamics and obstacle corridors. Warm-starting with the previous solution yields smooth, near-optimal trajectories without discrete motion libraries. Apollo’s Expectation–Maximisation planner alternates lateral smoothing with longitudinal speed optimisation, whereas Rastelli’s continuous-curvature scheme minimises jerk and curvature variation along Bézier splines. Both show that convex or near-convex formulations can meet real-time demands while overcoming the sub-optimality and roughness of sampling-based schemes, though at the cost of continual optimisation [163], [164].

Artificial Potential-field Navigation. Attractive and repulsive potentials characterise the goal as an energy well and obstacles as peaks, letting a robot follow the negative gradient in real time [165], [166]. Newton-style updates hasten escape from saddle points [167], and adaptive gain tun-

TABLE 4
Overview of representative rule-based motion-planning algorithms (§3.2.2).

Summary	Method	Publication	Core Architecture	Input Modality & Control Condition	Output Modality
<i>Car-following models</i>					
Car-following Models	IDM [154] IDM Roll-out Sampling [155]	Phys. Rev. E'00 CoRL'23	Closed-form ordinary-differential law Batched IDM roll-outs with cost ranking	Gap + Speed + Relative speed Gap + Speed + Relative speed	Longitudinal acceleration Minimum-cost acceleration
<i>Sampling-based planners</i>					
Sampling-based Random	RRT [156] RRT-Connect [157] RRT* / RRG [158], [159]	Tech. Rep.'98 ICRA'00 RSS'10 / IJRR'11	Tree search with random exploration Bi-directional RRT connection Rewiring optimal RRT for asymptotic optimality	State + Map + Obstacles State + Map + Obstacles State + Map + Obstacles	Feasible path Feasible path Near-optimal path
Sampling-based Deterministic	Spatiotemporal Lattice [160] Conformal Lattice [161] Discrete Terminal Manifold [162]	ICROS'09 ICRA'11 IJRR'12	Pre-tiled spatiotemporal lattice search Highway-aligned lattice search Polynomial library with A* search	Ego + State + Map Ego + State + Map Ego + State + Map	Trajectory Trajectory Time-critical trajectory
<i>Continuous optimisation</i>					
Continuous Optimisation	Apollo EM Planner [163] Continuous-Curvature Spline [164]	arXiv'18 IV'14	Alternating quadratic programming + dynamic programming Bézier-spline quadratic programming with jerk minimisation	Frenet path + Road corridor Obstacle corridor	Smooth trajectory Smooth trajectory
<i>Artificial potential-field navigation</i>					
Artificial Potential-Field	Classic APF [165], [166] Newton-PF [167] Hybrid Sigmoid-PF [168], [169] Torque-PD PF [170]	CISM'78 / IJRR'86 T-RO'06 Sensors'10 / IV'17 IV'15	Attractive-repulsive potential field Potential-field with Newton-based update Potential field with sigmoid blending Potential field within proportional-derivative steering	Goal pose + Obstacles Goal pose + Obstacles Goal pose + Obstacles Potential-field value	Steering force Steering force Steering command Steering torque

ing lessens oscillations on public roads [169]. Blending the field with sigmoid curves limits curvature spikes in dense traffic [168], while embedding the gradient in a torque-based proportional-derivative steering loop unifies motion planning with low-level control [170]. Although local minima persist, coupling potential-field guidance with higher-level sampling or MPC preserves rapid collision avoidance without forfeiting global optimality [171], [172].

Summary. Table 4 compares four major rule-based motion-planning paradigms. Several observations follow:

- ▶ Rule-based motion planners span car-following, sampling, continuous optimisation and potential-field families, balancing update rate, smoothness and global optimality while remaining easy to audit.
- ▶ Modern stacks fuse potential-field reflexes, discrete sampling diversity and MPC smoothing, yet modular design can miss global optima and fixed heuristics struggle under dense traffic shifts.

3.2.3 Search-based Planning

Search-based planners discretise the vehicle's high-dimensional, continuous state-space into a graph whose edges are motion primitives – short, pre-computed, kinematically feasible maneuvers. Classical graph-search techniques such as Dijkstra [179], [180] and the A* family [181], [182] then find the minimum-cost path according to heuristics that balance safety, smoothness, and progress. Vehicle constraints are embedded in the primitive library; Hybrid-State A* extends this idea by blending continuous headings with discrete cells to satisfy non-holonomic bicycle-model dynamics [183].

The approach offers strong optimality guarantees and explicit handling of traffic rules and obstacles, but suffers from the resolution-complexity trade-off: finer grids or larger graphs improve path quality and continuity yet raise computational load exponentially, jeopardising real-time performance. Recent work tackles this bottleneck with (i) model-predictive A* that employs relaxed cost-to-go maps for long-horizon searches in milliseconds [184], (ii) adaptive fidelity models that switch between simple longitudinal or drift dynamics to match task urgency [185], (iii) multi-heuristic search that fuses several admissible and inadmissible heuristics to accelerate exploration in cluttered layouts [186], and (iv) Task-and-Motion Planning hybrids that sample primitives from multiple local models while

maintaining optimality guarantees in nonlinear, unstable regimes [187]. Together these advances extend search-based planning from structured highway settings to complex urban and off-road scenarios while retaining its interpretable, graph-optimal foundation.

3.3 Interaction between Planning and Prediction

Interaction between behaviour planning and future prediction forms a feedback loop: the agent chooses actions while forecasting how all traffic will react. Tight coupling lets it pick manoeuvres that stay both safe and efficient. Research has advanced from passive log replay to fully interactive world models that respond online to ego actions (Fig. 3).

Generative Methods and Open-loop Regime. Recent generative approaches (e.g., DriveGAN [188], MagicDrive [189], and DriveDreamer [10]) narrow the sim-to-real gap by focusing on photorealism and synthesizing editable street-scene videos that substantially enrich training corpora; nevertheless, they merely replay pre-sampled futures without responding to online control inputs, thus confining research to a data-centric, open-loop paradigm that breaks the causal link between present actions and subsequent observations. TrafficGen [190] and LCTGen [191] generate traffic scenes from vector logs and natural-language prompts, respectively, while RealGen [192] retrieves and recombines template behaviours to create tag-specific or crash-critical scenarios. All three remain strictly open-loop, replaying fixed futures that ignore online control inputs. NAVSIM [193] shares this non-reactive paradigm, seeking only to refine open-loop metrics; it cannot inject rare events or alter traffic rules, offering merely quasi-closed-loop scores. These limitations draw growing criticism, as open-loop benchmarks can overstate safety and performance when an agent's actions never influence the futures being evaluated.

Auto-regressive World Models and Uncontrollable Closed-loop Regime. Auto-regressive driving world models [15], [46], [84], [85], [88], [89], [194]–[198] have quickly progressed from trajectory-only roll-outs to multi-sensor, long-horizon simulators that generate futures conditioned on ego actions, unifying prediction and planning in a single generative loop. This paradigm supplies cheap, diverse data, exposes planners to their own downstream consequences, and captures uncertainty more richly than fixed-log, open-loop corpora [15], [46], [199]. However, the latent physics are opaque: users cannot freely edit traffic rules, inject rare events, adjust replay speed, or verify safety guarantees,

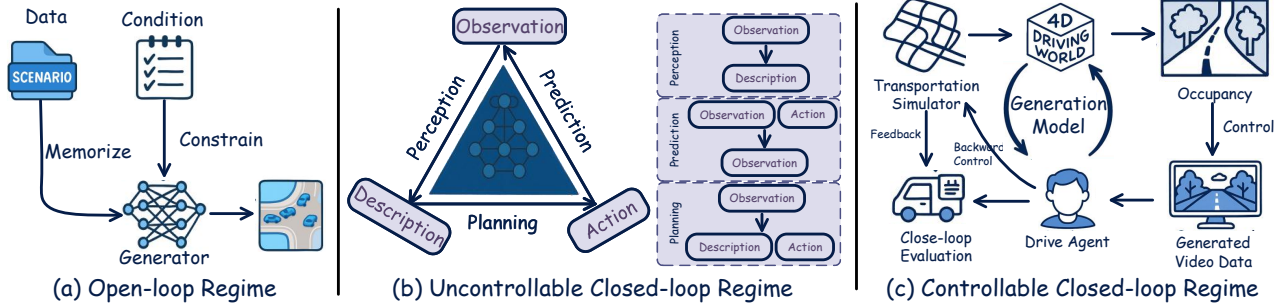


Fig. 3. **The evolution of interaction** (§3.3). (a) Open-loop regime synthesises scenes from logged data under static conditions; the generator memorises scenarios but never reacts to new actions. (b) Uncontrollable closed-loop regime unifies perception, prediction and planning in an auto-regressive loop, yet latent physics remain fixed, so users cannot inject rules or rare events. (c) Controllable closed-loop regime adds editable 4D worlds, occupancy control and feedback/backward signals, enabling a drive agent to interact safely with a fully testable simulator.

and compounding distribution drift still threatens reliability, leaving current systems in an uncontrollable closed-loop that hampers rigorous safety-critical evaluation [21].

Prior auto-regressive models relied primarily on image [15], [46], [84]. Recent work [85], [89] has integrated 3D occupancy grids into environmental modeling, providing a more detailed and robust representation of spatial dynamics. These grids enable accurate handling of occlusions and spatial relationships in dense urban scenes. However, their use in long-sequence video generation remains limited by the computational complexity of processing and maintaining large-scale 3D data over extended periods.

Controllable Closed-loop Regime. Research has progressed from script-driven traffic engines, through game-engine simulators with sensor realism, to neural and hybrid platforms that merge photoreal rendering with fully editable actor control. Early *microscopic engines* such as SUMO [200] exposed per-vehicle APIs for spawning, deletion and IDM/MOBIL/RL control, enabling fine-grained, reproducible experiments; Waymax [201] later accelerated log replay with JAX for rapid, sensor-free policy iteration, yet neither rendered raw sensor data. To fill this gap, CARLA [49] grafted Unreal-Engine visuals and configurable sensors onto a physics core, while MetaDrive [202] traded photoreal texture for procedural roads and kHz physics to support fast domain randomisation. Both deliver closed-loop images but still cover limited geographies and fall short of real-world visual fidelity, restricting direct transfer to models trained on natural data. *Neural-hybrid* simulators then appeared. UniSim [203] learns photoreal feature grids from a single drive, and OASim [204] re-poses vehicles with lighting-consistent implicit rendering, yet both remain bounded by their source clips. *Fidelity and interactivity* keeps expanding: Sky-Drive [205] adds socially aware multi-agent interactions; DriveArena [29] converts 2D traffic sketches to photoreal video; DrivingSphere [206] upgrades to 4D occupancy for geometrically accurate stress tests. The *LimSim family* scales closed-loop control to city networks. LimSim [207] offers distributed, scriptable traffic; LimSim++ [208] adds road-rule scripts and vision hooks; and the latest LIM-SIM Series [209] provides modular APIs for covering map topology, human-style bots and area-of-interest acceleration, allowing users to inject hazards, swap policies and tune metrics for rigorous, interactive safety validation.

Summary. The community has progressed from static, open-

loop datasets to fully interactive, high-fidelity simulators. Platforms that fuse controllable closed-loop dynamics with photoreal sensor generation pave the way for the next wave of behaviour-aware, safety-critical autonomous driving research. Several observations can be drawn:

- ▶ Closed-loop scores should complement or replace open-loop metrics to reveal true safety margins.
- ▶ Generative simulators reduce reliance on real-world collection by synthesising corner cases on demand.
- ▶ Tight planning–prediction integration inspires hybrid curricula: models alternate between logged supervision and interactive roll-outs, and share unified losses that couple trajectory forecasting with policy optimisation.

4 DATA AND TRAINING PARADIGMS

This section focuses on the methodologies for training models in autonomous driving, emphasizing self-supervised learning paradigms, pretraining strategies, and innovative approaches for data generation.

4.1 Self-Supervised Learning for World Models

Self-supervised world-model research for autonomous driving uses 2D images or raw LiDAR scans to automatically generate supervision, cutting 3D annotation costs. Rapid progress is now reshaping the field around 3D occupancy grids. Because dense voxel annotation is laborious, many groups pivoted to *cheaper* 2D supervision. RenderOcc [210], SelfOcc [211], OccNeRF [212] and related NeRF-style systems lift multi-view images into volumetric space, back-propagating depth or semantic losses so the network “hallucinates” occupancy; these image-only routes save annotation cost but lag LiDAR-centric baselines in fidelity and fine geometry. A *complementary branch* exploits the LiDAR stream itself: UnO [31] and EO [117] derive self-labels by contrasting predicted 4D fields with future scans, while RenderWorld [91], UniPAD [213], and PreWorld [82] couple differentiable rendering with multi-view cameras to fuse 2D texture and 3D structure; ViDAR [20] further aligns video patches to point clouds for stronger temporal motion priors. *Tokenisation and diffusion* bring a third flavour: COPilot4D [214] and BEVWorld [32] discretise multimodal data into vocabulary codes, then learn discrete diffusion to regenerate future scenes, capturing complex distributions without

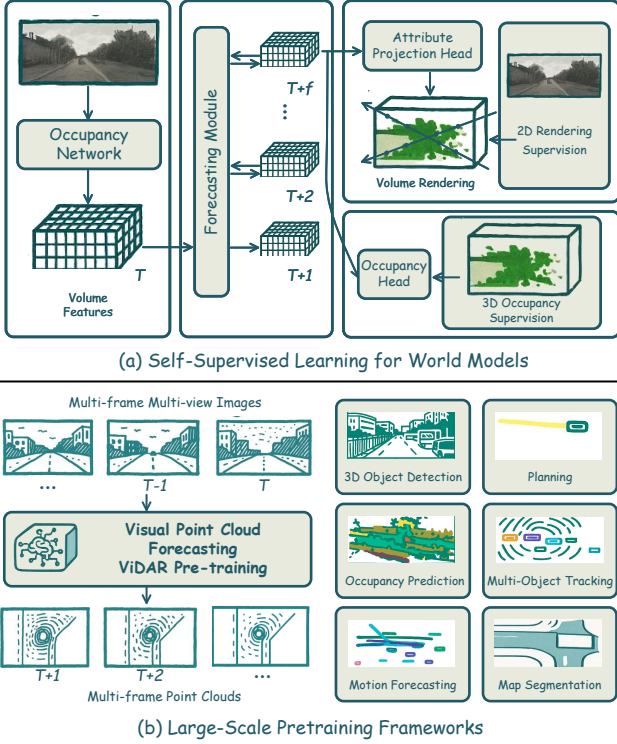


Fig. 4. (a) **Self-supervised world models** lift multi-view images into 3D volumes, forecast future grids, and learn from 2D renders plus occupancy cues, reducing labels (§4.1). (b) **Large-scale pre-training** on visual point-cloud sequences yields a single backbone that adapts to detection, tracking, mapping, occupancy, and planning (§4.2).

any human annotation, and AD-L-JEPA [215] eliminates both contrastive and generative heads, directly forecasting bird’s-eye embeddings for faster pre-training.

These techniques cut labeling costs, unify vision and geometry, and hint at closed-loop plan by letting a policy probe predicted futures. Current self-supervised occupancy models still face three key drawbacks. *Accuracy lags behind fully-supervised 3D/4D baselines* – NeRF-style pipelines, in particular, lose fine-scale detail. Volumetric rendering and diffusion inference incur *heavy compute and memory costs*, making long-horizon prediction slow and resource-hungry. Most methods predict only the current voxel grid; *principled, label-free 4D occupancy forecasting* remains largely unexplored. Looking ahead, key research directions include faster volumetric rendering, and tighter integration with downstream planners to verify that self-supervised grids truly improve safety rather than merely saving labels.

4.2 Large-Scale Pretraining Frameworks

A growing body of research argues that large-scale pre-training of world models is becoming the most economical path to robust autonomous driving. *Universal vision/multimodal frameworks* [20], [21], [32], [46], [82], [213], [216], [217] ingest millions of image-LiDAR sequences, encode them in a unified BEV or voxel space, and learn to forecast future occupancies or videos. Their strengths lie in rich spatio-temporal context, easy transfer to detection, segmentation, trajectory prediction and even planning, and drastic label-cost reduction. Weaknesses include heavy GPU

demand, sensitivity to camera calibration, and lingering reliance on heuristic heads (e.g., simple occupancy decoders). *LiDAR/occupancy-centric self-supervision* targets pure 3D geometry. Occupancy-MAE [218] masks voxels, AD-L-JEPA [215] reconstructs masked embeddings, and UnO [31] predicts continuous 4D occupancy fields from future point-cloud pseudo-labels. These methods excel at fine-grained geometry, learn on sparse data, and are sensor-agnostic, but they lack rich semantics and require precise temporal alignment. *Foundation-level generative world models* (e.g., Gaia-1 [15], Gaia-2 [58]) scale to hundreds of millions of frames, synthesize controllable multi-camera scenes, and couple generation with understanding. They promise closed-loop simulation and data augmentation, yet training cost and safety-critical evaluation remain open hurdles.

Collectively, research has progressed from early multimodal prediction networks, through *unified 4D pre-training pipelines*, to the first attempts at foundation generative models; at each stage the emphasis shifts from “perception only” to “perceive-predict-plan” while annotation demand falls. Hybrid systems are anticipated that fuse dense LiDAR self-supervision with the semantic richness and controllability of vision-centric foundation models. These systems are envisioned to provide task-aware, uncertainty-calibrated priors that can be fine-tuned online. Several open challenges remain: scalable temporal memory, principled safety validation, and energy-efficient training. If these hurdles are overcome, world-model pre-training is likely to become the standard backbone for all levels of autonomous-driving software.

4.3 Data Generation for Training

Large-scale autonomous-driving datasets are still dominated by natural logs collected with expensive fleets, yet §3.1 shows that modern world-model generators can manufacture much of what a learner needs. Early *image-centric* systems [10], [188] could only replay low-resolution clips, but the latest diffusion and Transformer models [14], [15], [46], [58] fuse text, HD-map, trajectory and sensor cues to paint photorealistic, action-conditioned street scenes that retain long-range temporal coherence. Their synthetic videos supplement rare night, rain and construction frames and feed directly into perception or closed-loop policy training. A *parallel stream* converts multi-view imagery or sparse LiDAR into structured representations before generation. BEV pipelines [22], [31], [33] first lift observations into a bird’s-eye lattice, then roll the lattice forward to harvest scene and intention labels at centimetre accuracy while filtering away distracting appearance noise. *Occupancy-grid diffusion* [17], [18] and *tokenised voxel Transformers* [85], [88] push this idea further: they stochastically sculpt 4D grids that obey physics, provide dense semantics and can be queried by planners for risk-aware cost volumes. Finally, *LiDAR-native approaches* [103], [106] learn score-based or latent denoisers on range images, recreating full sweeps with realistic sensor noise and occlusion artefacts; these meshes or point clouds supply geometry-heavy tasks (e.g., mapping, motion forecasting) without camera bias. Table 5 summarises representative methods and how their synthetic outputs feed into training.

Compared with hand-coded simulators, generator-based data pipelines offer three tangible benefits.

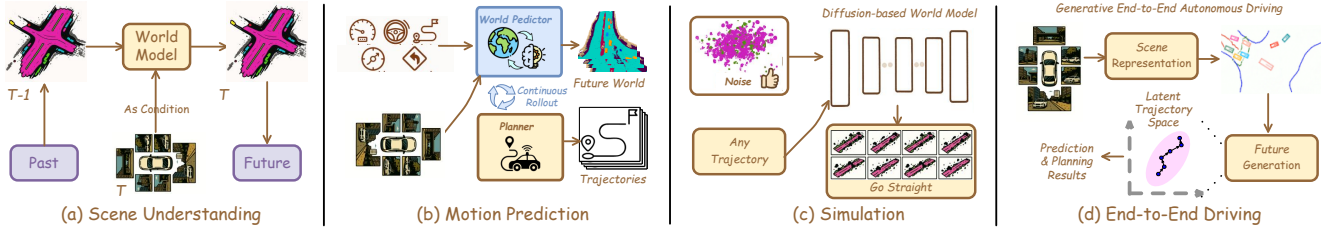


Fig. 5. **Application areas and tasks** (§5). (a) Scene understanding fuses multi-camera/LiDAR into a 4D BEV latent that updates every frame, giving precise geometry. (b) Motion prediction rolls latent forward under action cues, outputting collision fields for planners. (c) Simulation turns the generator into an editable 4D world where diffusion seeds rare traffic for safe closed-loop tests. (d) End-to-end driving joins perception, prediction and control in one autoregressive policy.

TABLE 5
Usage of data generation (§4.3).

Method	Usage of data generation
Generation reused for downstream tasks	
DriveDreamer-2 [37]	Generates user-customized videos from text prompts, and the authors discuss adding them to 3D detection training set.
BEVControl [43]	BEV sketches are converted to street-view images that fine-tune BEVFormer, boosting NDS by +1.29.
SimGen [47]	Simulator + real-layout images serve as augmentation, improving BEV detection & segmentation on nuScenes.
GAIA-2 [58]	Synthetic multi-camera videos feed Wayve’s offline perception & planning stack for training and safety validation.
Generation for self-training	
GEM [16]	Generates scenes from ego trajectory and DINO cues.
Vista [46]	High-fidelity video world model evaluated on generation metrics and RL reward.
GAIA-1 [15]	Demonstrates controllable scene synthesis.
DrivingWorld [64]	Video-GPT model measured by FID/FVD.
MiLA [59]	Targets long-horizon video synthesis for future training.
CoGen [57]	Produces controllable multi-view 3D-consistent scenes.

- ▶ **Coverage:** By conditioning on text or control commands, generators extrapolate to corner cases absent from logs.
- ▶ **Fidelity:** Multi-modal diffusion preserves cross-view consistency and metre-accurate depth, which classical game engines still struggle to match.
- ▶ **Efficiency:** Once trained they amortise fleet costs, allowing continuous data refresh through cheap sampling rather than fresh drives.

However, challenges remain: high-resolution diffusion is GPU-hungry; precise camera calibration is required for view-to-view consistency; and safety assessment of purely synthetic curricula is still an open research problem. Nevertheless, data generation has evolved from a niche augmentation trick to a central pillar of autonomous-driving training pipelines, and future hybrids that blend LiDAR-tight geometry with image-level semantics are expected to yield even richer corpora for end-to-end learning.

5 APPLICATION AREAS AND TASKS

Through the integration of world models, autonomous driving systems have made progress in tasks such as scene understanding, motion prediction, simulation, and end-to-end driving, demonstrating greater reliability and adaptability.

5.1 Scene Understanding

High-fidelity 3D reconstruction is vital, but real sensors are noisy and costly to label. World models answer by compressing multi-camera and LiDAR streams into a unified spatio-temporal latent that continuously refreshes as new frames arrive. *Early 4D pre-training* shows that one memory state can support detection, mapping and tracking without task-specific heads [21]. Subsequent *BEV-centric tokenisers*

project all modalities into a compact bird’s-eye lattice; decoding that lattice back to pixels or point clouds yields high-resolution semantics and largely removes the need for manual fusion heuristics [32]. *A parallel line* predicts dense 3D occupancies instead of bounding boxes [90], giving planners free-space priors that remain topologically consistent over seconds rather than frames [18], [85]. *Physical realism* continues to rise as neural volumetric splats attach radiance and density to each voxel, turning the map into a differentiable oracle for visibility or risk gradients [217], [219]. These advances collapse sensor boundaries, cut annotation budgets, and make scene understanding an anticipatory rather than reactive module; the price is GPU memory and still-uncertain safety certificates for learned geometry.

5.2 Motion Prediction

Future-state inference has moved from extrapolating agent boxes to rolling the latent world forward. Diffusion-based generators evolve the entire scene as a 4D occupancy video that enforces basic physical-consistency losses, allowing planners to clamp candidate ego trajectories and query collision risk in milliseconds [18]. Tokenised video models extend horizons beyond a minute while preserving fine intent cues, widening the temporal window for congestion management and logistics scheduling [220]. Vision-centric hybrids link these 4D forecasts to an end-to-end planner, delivering action-controllable occupancy roll-outs that bypass separate mapping stages [88]. Behaviour realism improves when multi-agent personalities are embedded inside the world; latent “traffic bots” yield socially plausible manoeuvres without brittle lane-change heuristics [197], [198]. The unified latent now integrates map topology, social norms, and kinematics, delivering probability fields that planners can sample or edit instead of juggling disparate trajectory sets. Remaining challenges lie in compute-heavy diffusion roll-outs and the calibration of epistemic uncertainty when imagined futures drift far from training data.

5.3 Simulation

Traditional game-engine simulators cannot keep pace with the diversity and rare traffic cases. Generative world models fill that gap by producing controllable, multi-modal replicas of the road. Latent-diffusion frameworks synthesize multi-camera sequences with pixel-level realism and cross-view depth consistency, strong enough for perception-regression tests and data augmentation [15], [46], [58]. Cascade pipelines further blend simulator geometry with real

TABLE 6

4D scene generation comparison (§6.2). Metrics reported for OccSora [18] vs DynamicCity [17] on CarlaSC [97] and Occ3D-Waymo [83], in both 2D and 3D evaluation spaces.

Dataset	Method	#Frames	2D Metrics				3D Metrics			
			IS↑	FID↓	KID↓	P↑	R↑	IS↑	FID↓	KID↓
CarlaSC	OccSora [18]	16	1.030	28.55	0.008	0.224	0.010	2.257	1559	52.72
	DynamicCity [17]		1.040	12.94	0.002	0.307	0.018	2.331	354.2	19.10
Occ3D-Waymo	OccSora [18]	16	1.005	42.53	0.049	0.654	0.004	3.129	3140	12.20
	DynamicCity [17]		1.010	36.73	0.001	0.705	0.015	3.206	1806	77.71

TABLE 7

Point cloud forecasting performance on OpenScene [221] mini val set (§6.3).

Method	Chamfer Distance (m^2) ↓						
	0.5s	1.0s	1.5s	2.0s	2.5s	3.0s	Avg.
ViDAR [20]	1.34	1.43	1.51	1.60	1.71	1.86	1.58
DFIT-OccWorld-O [86]	0.38	0.72	0.74	0.75	0.79	0.86	0.70
DFIT-OccWorld-V [86]	0.40	0.75	0.78	0.83	0.89	0.90	0.76

video priors, shrinking the sim-to-real gap and measurably improving BEV detectors when synthetic clips are mixed into training corpora [14], [47]. Geometry-first approaches generate long 4D occupancy volumes, supplying verification tools with dense physical states rather than mere imagery [18], [60], [95]. High-fidelity platforms now close the interaction loop, letting policies influence rendered frames each step and revealing covariate-shift failures before road deployment [29], [203], [206]. However, GPU cost and regulatory acceptance remain hurdles.

5.4 End-to-End Driving

End-to-end pipelines once mapped pixels directly to control signals through black-box regression; world models now provide the memory, foresight and language hooks that make such systems transparent and data-efficient. Generative architectures recast driving as next-token prediction in a multimodal language, producing future frames and waypoint plans that lower collision rates compared with deterministic baselines [22], [127]. Large closed-loop models integrate perception, prediction and control inside a single autoregressive policy, evaluating imagined futures every control cycle to boost rule compliance and ride comfort [196]. Language-vision transformers extend controllability: a single sequence model now obeys natural-language directives like “yield at the zebra crossing, then merge” without extra planners [127], [191]. Lightweight augmentations place a predictive head in front of imitation layers; gradients through imagined roll-outs have been reported to reduce real-world data requirements and expose intermediate occupancy maps for audit [129], [222]. Token limits and long-horizon coherence remain open issues.

6 PERFORMANCE COMPARISON

This section presents an evaluation of world models for autonomous driving across tasks and metrics. Based on discussions in §5, representative algorithms are benchmarked to provide empirical evidence of their strengths and limitations.

6.1 Evaluation Platforms and Benchmarks

CarlaSC. CarlaSC [97] is a synthetic dataset generated via CARLA, offering 4D occupancy at $128 \times 128 \times 8$ resolution within a $25.6m \times 25.6m \times 3m$ volume around the ego-vehicle.

NuScenes. nuScenes [36] contains 1,000 scenes split into 700 train, 150 val, and 150 test. It includes six RGB cameras (360°) and 32-beam LiDAR with centimeter-level accuracy.

Occ3D-nuScenes. Occ3D-nuScenes [83] is built from nuScenes with 700 training and 150 validation sequences, each with ~ 40 frames at 2Hz.

Occ3D-Waymo. Occ3D-Waymo [83] is based on Waymo [38], with 798 training and 202 validation sequences, each ~ 200 frames at 10Hz, covering 17 semantic classes.

OpenScene. OpenScene [221], from nuPlan [223], spans over 120 hours across four cities with 600,000+ frames. It uses eight cameras and five LiDARs. OpenScene-mini has 5,392 train and 8,729 val frames.

6.2 4D Scene Generation

4D Scene Generation refers to the task of synthesizing temporally coherent 3D scene sequences that evolve over time, effectively capturing both spatial and temporal dynamics.

Metrics. For 4D Scene Generation, both 2D and 3D perceptual quality metrics are employed: (i) Inception Score (IS) ↑; (ii) Fréchet Inception Distance (FID) ↓; (iii) Kernel Inception Distance (KID) ↓; (iv) Precision (P) ↑; (v) Recall (R) ↑.

Results. To evaluate the effectiveness of DynamicCity [17] in 4D scene generation, comparisons are conducted against OccSora [18] on the Occ3D-Waymo [83] and CarlaSC [97] benchmarks. As reported in Table 6, IS, FID, KID, P, and R are measured in both 2D and 3D spaces. Across both benchmarks and evaluation spaces, DynamicCity consistently delivers higher perceptual quality (IS, FID) and stronger fidelity-diversity trade-offs, validating its effectiveness in generating realistic 4D scenes. Looking forward, research is converging on geometry-consistent 4D diffusion with text/trajectory/physics conditioning and unified RGB-depth-occupancy rendering to support interactive simulators.

6.3 Point Cloud Forecasting

Point cloud forecasting is a self-supervised task that predicts future point clouds from past observations, traditionally using range-image projections processed by 3D convolutions or LSTMs while explicitly modeling sensor motion.

Metrics. Chamfer Distance (CD) ↓ are employed as evaluation metric for point cloud forecasting. CD measures the similarity between a predicted point cloud and its ground-truth counterpart. Lower CD values indicate higher fidelity in capturing the true spatial distribution of points.

Results. Table 7 shows that both DFIT-OccWorld variants substantially outperform the ViDAR baseline at every forecast horizon. DFIT-OccWorld-O trims mean CD to $0.70m^2$ and stays ahead of ViDAR across all horizons; the V-variant follows at $0.76m^2$, and the gap widens as lead time grows. The field is shifting from range-image CNN/LSTM to token-based diffusion, leveraging image priors and physics constraints to sustain long-horizon precision.

TABLE 8
4D occupancy forecasting on the Occ3D-nuScenes [83] dataset (§6.4). Aux. Sup. denotes auxiliary supervision apart from the ego trajectory. Avg. denotes the average performance of that in 1s, 2s, and 3s.

Method	Input	Aux. Sup.	mIoU ↑				IoU ↑			
			1s	2s	3s	Avg.	1s	2s	3s	Avg.
Copy&Paste	3D-Occ	None	14.91	10.54	8.52	11.33	24.47	19.77	17.31	20.52
OccWorld [85]	3D-Occ	None	25.78	15.14	10.51	17.14	34.63	25.07	20.18	26.63
RenderWorld [91]	3D-Occ	None	28.69	18.89	14.83	20.80	37.74	28.41	24.08	30.08
OccLlAMA-O [89]	3D-Occ	None	25.05	19.49	15.26	19.93	34.56	28.53	24.41	29.17
DOME-O [95]	3D-Occ	None	35.11	25.89	20.29	27.10	43.99	35.36	29.74	36.36
DFIT-OccWorld-O [86]	3D-Occ	None	31.68	21.29	15.18	22.71	40.28	31.24	25.29	32.27
TPVFormer [224]:Lidar+OccWorld-T [85]	Camera	Semantic LiDAR	4.68	3.36	2.63	3.56	9.32	8.23	7.47	8.34
TPVFormer [224]+SelfOcc [211]+OccWorld-S [85]	Camera	None	0.28	0.26	0.24	0.26	5.05	5.01	4.95	5.00
OccWorld-F [89]	Camera	None	8.03	6.91	3.54	6.16	23.62	18.13	15.22	18.99
OccLlAMA-F [89]	Camera	None	10.34	8.66	6.98	8.66	25.81	23.19	19.97	22.99
RenderWorld [91]	Camera	None	2.83	2.55	2.37	2.58	14.61	13.61	12.98	13.73
DOME-F [95]	Camera	None	24.12	17.41	13.24	18.25	35.18	27.90	23.435	28.84
DFIT-OccWorld [86]	Camera	3D-Occ	13.38	10.16	7.96	10.50	19.18	16.85	15.02	17.02

TABLE 9
Motion planning on the nuScenes [36] dataset (§6.5). Aux. Sup. denotes auxiliary supervision apart from the ego trajectory.

Method	Input	Aux. Sup.	L2 (m) ↓				Collision Rate (%) ↓			
			1s	2s	3s	Avg.	1s	2s	3s	Avg.
NMP [133]	LiDAR	Box & Motion	0.53	1.25	2.67	1.48	0.04	0.12	0.87	0.34
FF [134]	LiDAR	Freespace	0.55	1.20	2.54	1.43	0.06	0.17	1.07	0.43
EO [117]	LiDAR	Freespace	0.67	1.36	2.78	1.60	0.04	0.09	0.88	0.33
ST-P3 [27]	Camera	Map & Box & Depth	1.33	2.11	2.90	2.11	0.23	0.62	1.27	0.71
UniAD [225]	Camera	Map & Box & Motion & Tracklets & Occ	0.48	0.96	1.65	1.03	0.05	0.17	0.71	0.31
UniAD+DriveWorld [21]	Camera	Map & Box & Motion & Tracklets & Occ	0.34	0.67	1.07	0.69	0.04	0.12	0.41	0.19
DriveDreamer [10]	Camera	Map & Box & Motion	-	-	-	0.29	-	-	-	0.15
GenAD [22]	Camera	Map & Box & Motion	0.36	0.83	1.55	0.91	0.06	0.23	1.00	0.43
OccWorld-T [85]	Camera	Semantic LiDAR	0.54	1.36	2.66	1.52	0.12	0.40	1.59	0.70
OccWorld-S [85]	Camera	None	0.67	1.69	3.13	1.83	0.19	1.28	4.59	2.02
Drive-OcWorld [88]	Camera	None	0.32	0.75	1.49	0.85	0.05	0.17	0.64	0.29
ViDAR [20]	Camera	None	-	-	-	0.91	-	-	-	0.23
OccWorld-F [89]	Camera	Occ	0.45	1.33	2.25	1.34	0.08	0.42	1.71	0.73
OccLlAMA-F [89]	Camera	Occ	0.38	1.07	2.15	1.20	0.06	0.39	1.65	0.70
RenderWorld [91]	Camera	Occ	0.48	1.30	2.67	1.48	0.14	0.55	2.23	0.97
DFIT-OcWorld-V [86]	Camera	Occ	0.42	1.14	2.19	1.25	0.09	0.19	1.37	0.55
OccWorld [85]	3D-Occ	None	0.43	1.08	1.99	1.17	0.07	0.38	1.35	0.60
RenderWorld [91]	3D-Occ	None	0.35	0.91	1.84	1.03	0.05	0.40	1.39	0.61
OccLlAMA-O [89]	3D-Occ	None	0.37	1.02	2.03	1.14	0.04	0.24	1.20	0.49
DFIT-OcWorld-O [86]	3D-Occ	None	0.38	0.96	1.73	1.02	0.07	0.39	0.90	0.45

6.4 4D Occupancy Forecasting

This subsection examines models' capabilities to perceive and predict dynamic scenes, focusing on how moving objects and their interactions evolve over time.

Metrics. The evaluation of occupancy forecasting relies on mIoU and IoUs to gauge how accurately each future frame's semantic occupancy is recovered, while placing additional emphasis on temporal accuracy and consistency across multiple time horizons (e.g., 1s, 2s, 3s).

Results. Table 8 summarizes the 4D occupancy forecasting performance on Occ3D-nuScenes [83], where predictions for 1s, 2s, and 3s into the future are assessed via mIoU and IoU. Notably, DOME-O attains state-of-the-art results (27.10% mIoU and 36.36% IoU), surpassing baseline methods such as OccWorld and RenderWorld by substantial margins. Even the purely camera-based DOME-F variant remains highly competitive, reflecting the model's robustness in scenarios without direct 3D occupancy supervision. Future advances target tokenised or diffusion backbones that accept language or trajectory prompts and camera-only pipelines that cut LiDAR cost while keeping real-time viability.

6.5 Motion planning

Motion planning rapidly generates collision-free, energy-aware trajectories by considering obstacles, road layout, and surrounding vehicles, promoting safety and efficiency.

Metrics. The evaluation of motion planning centers on key aspects such as L2 error and collision rate. L2 error quantifies how closely a planned trajectory tracks the reference or desired path, while collision rate measures the frequency of unsafe interactions with obstacles.

Results. Table 9 presents a quantitative comparison of motion planning methods on the nuScenes [36] dataset. End-to-end planners (e.g., UniAD [225]) achieve the lowest average L2 error and collision rate when trained with rich map, box and motion labels. Occupancy-centric methods (e.g., OccWorld [85], RenderWorld [91], DFIT-OcWorld [86]) retain competitive accuracy while discarding most auxiliary supervision, especially in camera-only setups. RenderWorld further achieves a ~34% reduction in collision rate over a 3-second horizon compared to OccWorld, indicating safer long-horizon forecasts. Overall, the table highlights how both occupancy-centric and end-to-end solutions excel at generating precise, collision-free paths, with top-performing models striking an effective balance between minimal supervision and accurate motion forecasting.

7 FUTURE RESEARCH DIRECTIONS

This section surveys four frontier directions – self-supervised learning, multi-modal fusion, advanced simulation, and efficient architectures – that aim to reduce label dependence, sharpen perception and planning, boost simulation realism, and enable resource-aware deployment.

7.1 Self-Supervised World Models

Self-supervision has already proven that large amounts of annotated data are useful but not indispensable.

Reducing Label Dependency. Upcoming work is expected to couple cross-modal reconstruction (images \leftrightarrow LiDAR \leftrightarrow occupancy) with strong physics-based consistency losses. By letting each sensor stream synthesize or critique the others, a single model can refine depth, motion, and semantics

without ever seeing a hand-drawn box. Generative objectives (e.g., long-horizon video rollout, stochastic occupancy completion, or latent LiDAR synthesis) will serve as ‘free’ supervision signals that capture rare weather, lighting, and traffic events. Combined with lightweight on-device distillation and sparse activation routing, these techniques promise to slash annotation budgets while keeping the model small enough for automotive hardware.

Exploring Unlabeled Data Potential. Beyond saving labels, the frontier is to *unlock the structure* hidden in the ocean of raw fleet logs. Self-supervised world models will (i) maintain a long-term memory that adapts online yet respects safety guarantees, (ii) roll imagined futures to train planners entirely in latent space, and (iii) estimate aleatoric and epistemic uncertainty on-the-fly so that risk grows when the model drifts away from familiar distributions. Coupling these world models with reinforcement learning agents turns every kilometre (real or simulated) into a self-improvement step, gradually building a driving policy that requires fewer interventions and generalises across cities.

7.2 Multi-Modal World Models

Packing images, point clouds, and BEV cues into a single latent already lifts perception, prediction, and planning. The next wave seeks universal embeddings that ingest any sensor (e.g., camera, LiDAR, radar, event, or thermal) without hand-tuned adapters. Three paths emerge: (i) ultra-compact cross-modal tokenisers that keep geometry and texture yet run on car-grade GPUs; (ii) self-aligning schedulers that weld asynchronous packets into causally consistent world states; (iii) curriculum objectives uniting differentiable rendering, language grounding, and physics-aware roll-outs so semantics, intent, and constraints co-evolve. Realising these goals would give vehicles a single, continuously refreshed memory that streamlines control, supports life-long adaptation, and sustains robustness under sensor degradation.

7.3 Advanced Simulation

Physics Engine. Physics-aware generation steers autonomous-driving simulators. DrivePhysica aligns ego/world frames, injects 3D flows, and applies box-guided occlusion, yielding multi-camera videos [50]. Future platforms fuse diffusion world models with differentiable rigid, soft, fluid, and thermal solvers in one loop. Diffusion priors sketch 4D occupancy while the solver enforces Newtonian laws, ensuring validity and gradients that reveal traction loss, drag, or sensor occlusion before deployment.

Cross-Scenario Generalization. Next-generation simulators will synthesize domain-agnostic worlds spanning cities, seasons, and driving styles. Interaction corpora toughen policies in unseen regions, while text-guided generators inject rare hazards and cultural norms to push controllers beyond sensor priors. Hybrid neural-physics engines let weather, lighting, and dynamics be tuned on the fly, unifying perception tests, policy search, and safety proofs. The goal is a fully differentiable sandbox where traffic rules, multi-agent uncertainty, and physics co-evolve, enabling auto-curricula and online co-training to shorten real-world validation.

Real-World Validation. Modern volumetric rendering, panoramic synthesis, and cross-modal alignment let simulators mirror city traffic with centimetre geometry, photorealism across weather, and agent motion. This fidelity boosts detector pre-training, fortifies long-horizon planners, and exposes corner-case failures before road tests, while physics-based sensors and diffusion controllers keep synthetic trajectories feasible. Continuous loops align simulated outputs with fleet telemetry, producing scalable, balanced scenarios that accelerate research and validation across perception, prediction, and control.

Diffusion-based Generation. Diffusion-based world modelling is converging toward unified generators that synthesise kilometre-long journeys while remaining tractable on embedded hardware. Progress unfolds along four axes. First, spatial coverage widens from single images to volumetric 4D roll-outs, giving planners seconds of geometry and exposing long-horizon corner cases. Second, richer conditioning blends panoramic cameras, text, motion plans, and physics priors so each sample obeys traffic rules, weather, and social etiquette. Third, efficiency improves through tokenised latents, causal masking, and hierarchical caches that cut memory and latency without sacrificing detail. Fourth, interactive editing enables on-the-fly swaps of agents, lanes, or illumination, turning the generator into a reusable testbed. Paired with emerging perception-plus-control benchmarks, these strands point toward self-improving simulators that shorten validation cycles, reduce data costs, and hasten autonomous-driving deployment.

7.4 Efficient World Models

Looking forward, efficient world models will rely on lean, latency-aware backbones that fuse sensing, prediction, and control in a single sweep. One shared feature reservoir – drawing jointly on vision, depth, and map cues – will serve every downstream head, eliminating costly re-projection. Lightweight language adapters will weave route guidance and traffic regulations into this common space. Scene motion will be roughed out as coarse flow; only ambiguous regions will be up-sampled into dense volumes, slashing computation. Multi-scale grids will stream context before zooming into high-detail regions around dynamic agents, conserving memory. Capacity-elastic layers will monitor feature entropy and activate deeper blocks only when congestion rises, sustaining real-time performance on modest vehicle GPUs. Coupled with edge quantisation and federated updates, these systems will learn continually from fleet data while respecting power, bandwidth, and privacy limits – bringing scalable, safety-critical autonomy within tangible reach.

8 CONCLUSION

World models have rapidly become a cornerstone for autonomous driving, enabling deeper integration among perception, prediction, and decision-making. Recent advances in multi-modal fusion unify data from cameras, LiDAR, and other sensors, while self-supervised learning and large-scale pretraining reduce dependence on annotated datasets. Generative methods, particularly diffusion-based approaches,

now facilitate diverse synthetic data for long-tail scenarios, enhancing model robustness in rare or extreme conditions. New frameworks tightly couple motion prediction with planning algorithms, moving toward closed-loop paradigms that promise safer, more adaptive navigation. As sensing technologies evolve and cross-domain datasets proliferate, world models are poised to become even more integral to the reliable, large-scale deployment of next-generation autonomous driving systems.

REFERENCES

- [1] D. J. Fagnant and K. Kockelman, "Preparing a nation for autonomous vehicles: opportunities, barriers and policy recommendations," *Transp. Res. Part A: Policy Pract.*, vol. 77, pp. 167–181, 2015. [1](#)
- [2] W. H. Organization, *Global status report on road safety 2018*. World Health Organization, 2019. [1](#)
- [3] L. Liu, S. Lu, R. Zhong, B. Wu, Y. Yao, Q. Zhang, and W. Shi, "Computing systems for autonomous driving: State of the art and challenges," *IEEE Internet Things J.*, vol. 8, pp. 6469–6486, 2020. [1](#)
- [4] S. Grigorescu, B. Trasnea, T. T. Cocias, and G. Macesanu, "A survey of deep learning techniques for autonomous driving," *J. Field Robot.*, vol. 37, pp. 362 – 386, 2019. [1](#)
- [5] A. Furda and L. Vlacic, "Enabling safe autonomous driving in real-world city traffic using multiple criteria decision making," *IEEE Intell. Transp. Syst. Mag.*, vol. 3, pp. 4–17, 2011. [1](#)
- [6] W. Schwarting, J. Alonso-Mora, and D. Rus, "Planning and decision-making for autonomous vehicles," *Annu. Rev. Control Robot. Auton. Syst.*, vol. 1, no. 1, pp. 187–210, 2018. [1, 7](#)
- [7] S. Manivasagam, S. Wang, K. Wong, W. Zeng, M. Sazanovich, S. Tan, B. Yang, W.-C. Ma, and R. Urtasun, "Lidarsim: Realistic lidar simulation by leveraging the real world," in *Proc. IEEE Conf. Comput. Vis. Pattern Recognit.*, 2020, pp. 11167–11176. [1, 6](#)
- [8] S. Li, "Research on the application of machine learning in the real time decision system of autonomous vehicles," *Front. Comput. Intell. Syst.*, 2023. [1](#)
- [9] D. Bogdoll, N. Ollick, T. Joseph, S. Pavlitska, and J. M. Zöllner, "Umad: Unsupervised mask-level anomaly detection for autonomous driving," *arXiv preprint arXiv:2406.06370*, 2024. [1](#)
- [10] X. Wang, Z. Zhu, G. Huang, X. Chen, J. Zhu, and J. Lu, "Drivenreamer: Towards real-world-drive world models for autonomous driving," in *Proc. Eur. Conf. Comput. Vis.* Springer, 2024, pp. 55–72. [1, 2, 3, 4, 9, 11, 14](#)
- [11] J. Ding, Y. Zhang, Y. Shang, Y. Zhang, Z. Zong, J. Feng, Y. Yuan, H. Su, N. Li, N. Sukiennik *et al.*, "Understanding world or predicting future? a comprehensive survey of world models," *arXiv preprint arXiv:2411.14499*, 2024. [1, 3](#)
- [12] D. Ha and J. Schmidhuber, "World models," *arXiv preprint arXiv:1803.10122*, 2018. [1, 3](#)
- [13] L. Qian, X. Xu, Y. Zeng, and J. Huang, "Deep, consistent behavioral decision making with planning features for autonomous vehicles," *Electronics*, 2019. [1, 2, 7](#)
- [14] X. Li, Y. Zhang, and X. Ye, "Drivingdiffusion: Layout-guided multi-view driving scenarios video generation with latent diffusion model," in *Proc. Eur. Conf. Comput. Vis.* Springer, 2024, pp. 469–485. [1, 3, 4, 11, 13](#)
- [15] A. Hu, L. Russell, H. Yeo, Z. Murez, G. Fedoseev, A. Kendall, J. Shotton, and G. Corrado, "Gaia-1: A generative world model for autonomous driving," *arXiv preprint arXiv:2309.17080*, 2023. [1, 4, 9, 10, 11, 12](#)
- [16] M. Hassan, S. Stapf, A. Rahimi, P. Rezende, Y. Haghghi, D. Brüggemann, I. Katircioglu, L. Zhang, X. Chen, S. Saha *et al.*, "Gem: A generalizable ego-vision multimodal world model for fine-grained ego-motion, object dynamics, and scene composition control," in *Proc. IEEE Conf. Comput. Vis. Pattern Recognit.*, 2024. [1, 4, 12](#)
- [17] H. Bian, L. Kong, H. Xie, L. Pan, Y. Qiao, and Z. Liu, "Dynamiccity: Large-scale 4d occupancy generation from dynamic scenes," in *Proc. Int. Conf. Learn. Represent.*, 2025. [1, 5, 6, 11, 13](#)
- [18] L. Wang, W. Zheng, Y. Ren, H. Jiang, Z. Cui, H. Yu, and J. Lu, "Occsora: 4d occupancy generation models as world simulators for autonomous driving," *arXiv preprint arXiv:2405.20337*, 2024. [1, 2, 5, 6, 11, 12, 13](#)
- [19] P. Wang, S. Gao, L. Li, S. Cheng, and H. xia Zhao, "Research on driving behavior decision making system of autonomous driving vehicle based on benefit evaluation model," *Arch. Transp.*, 2020. [1](#)
- [20] Z. Yang, L. Chen, Y. Sun, and H. Li, "Visual point cloud forecasting enables scalable autonomous driving," in *Proc. IEEE Conf. Comput. Vis. Pattern Recognit.*, 2024, pp. 14673–14684. [1, 3, 5, 6, 10, 11, 13, 14](#)
- [21] C. Min, D. Zhao, L. Xiao, J. Zhao, X. Xu, Z. Zhu, L. Jin, J. Li, Y. Guo, J. Xing *et al.*, "Driveworld: 4d pre-trained scene understanding via world models for autonomous driving," in *Proc. IEEE Conf. Comput. Vis. Pattern Recognit.*, 2024, pp. 15522–15533. [1, 5, 6, 10, 11, 12, 14](#)
- [22] W. Zheng, R. Song, X. Guo, C. Zhang, and L. Chen, "Genad: Generative end-to-end autonomous driving," in *Proc. Eur. Conf. Comput. Vis.* Springer, 2025, pp. 87–104. [1, 3, 4, 5, 11, 13, 14](#)
- [23] Z. Zhu, X. Wang, W. Zhao, C. Min, N. Deng, M. Dou, Y. Wang, B. Shi, K. Wang, C. Zhang *et al.*, "Is sora a world simulator? a comprehensive survey on general world models and beyond," *arXiv preprint arXiv:2405.03520*, 2024. [1](#)
- [24] Y. Guan, H. Liao, Z. Li, J. Hu, R. Yuan, Y. Li, G. Zhang, and C. Xu, "World models for autonomous driving: An initial survey," *IEEE Trans. Intell. Veh.*, 2024. [1, 3](#)
- [25] A. Fu, Y. Zhou, T. Zhou, Y. Yang, B. Gao, Q. Li, G. Wu, and L. Shao, "Exploring the interplay between video generation and world models in autonomous driving: A survey," *arXiv preprint arXiv:2411.02914*, 2024. [1](#)
- [26] G. Zhao, C. Ni, X. Wang, Z. Zhu, X. Zhang, Y. Wang, G. Huang, X. Chen, B. Wang, Y. Zhang *et al.*, "Drivenreamer4d: World models are effective data machines for 4d driving scene representation," in *Proc. IEEE Conf. Comput. Vis. Pattern Recognit.*, 2025. [2, 3, 4](#)
- [27] S. Hu, L. Chen, P. Wu, H. Li, J. Yan, and D. Tao, "St-p3: End-to-end vision-based autonomous driving via spatial-temporal feature learning," in *Proc. Eur. Conf. Comput. Vis.* Springer, 2022, pp. 533–549. [2, 3, 7, 8, 14](#)
- [28] S. Casas, A. Sadat, and R. Urtasun, "Mp3: A unified model to map, perceive, predict and plan," in *Proc. IEEE Conf. Comput. Vis. Pattern Recognit.*, 2021, pp. 14403–14412. [2, 5, 7, 8](#)
- [29] X. Yang, L. Wen, Y. Ma, J. Mei, X. Li, T. Wei, W. Lei, D. Fu, P. Cai, M. Dou *et al.*, "Drivearena: A closed-loop generative simulation platform for autonomous driving," *arXiv preprint arXiv:2408.00415*, 2024. [2, 10, 13](#)
- [30] D. Ha and J. Schmidhuber, "Recurrent world models facilitate policy evolution," *Advances in neural information processing systems*, vol. 31, 2018. [3](#)
- [31] B. Agro, Q. Sykora, S. Casas, T. Gilles, and R. Urtasun, "Uno: Unsupervised occupancy fields for perception and forecasting," in *Proc. IEEE Conf. Comput. Vis. Pattern Recognit.*, 2024, pp. 14487–14496. [3, 4, 5, 10, 11](#)
- [32] Y. Zhang, S. Gong, K. Xiong, X. Ye, X. Tan, F. Wang, J. Huang, H. Wu, and H. Wang, "Bevworld: A multimodal world model for autonomous driving via unified bev latent space," *arXiv preprint arXiv:2407.05679*, 2024. [3, 4, 10, 11, 12](#)
- [33] A. Hu, Z. Murez, N. Mohan, S. Dudas, J. Hawke, V. Badri-narayanan, R. Cipolla, and A. Kendall, "Fiery: Future instance prediction in bird's-eye view from surround monocular cameras," in *Proc. IEEE Int. Conf. Comput. Vis.*, 2021, pp. 15273–15282. [3, 4, 5, 11](#)
- [34] A. Hu, G. Corrado, N. Griffiths, Z. Murez, C. Gurau, H. Yeo, A. Kendall, R. Cipolla, and J. Shotton, "Model-based imitation learning for urban driving," in *Proc. Adv. Neural Inf. Process. Syst.*, vol. 35, 2022, pp. 20703–20716. [3, 4, 5, 7](#)
- [35] A. Popov, A. Degirmenci, D. Wehr, S. Hegde, R. Oldja, A. Kamenev, B. Douillard, D. Nistér, U. Müller, R. Bhargava *et al.*, "Mitigating covariate shift in imitation learning for autonomous vehicles using latent space generative world models," *arXiv preprint arXiv:2409.16663*, 2024. [3, 4](#)
- [36] H. Caesar, V. Bankiti, A. H. Lang, S. Vora, V. E. Liong, Q. Xu, A. Krishnan, Y. Pan, G. Baldan, and O. Beijbom, "nuscenes: A multimodal dataset for autonomous driving," in *Proc. IEEE Conf. Comput. Vis. Pattern Recognit.*, 2020, pp. 11621–11631. [4, 6, 7, 13, 14](#)
- [37] G. Zhao, X. Wang, Z. Zhu, X. Chen, G. Huang, X. Bao, and X. Wang, "Drivenreamer-2: Llm-enhanced world models for diverse driving video generation," in *AAAI Conf. Artif. Intell.*, vol. 39, no. 10, 2025, pp. 10412–10420. [3, 4, 12](#)

[38] P. Sun, H. Kretzschmar, X. Dotiwalla, A. Chouard, V. Patnaik, P. Tsui, J. Guo, Y. Zhou, Y. Chai, B. Caine *et al.*, "Scalability in perception for autonomous driving: Waymo open dataset," in *Proc. IEEE Conf. Comput. Vis. Pattern Recognit.*, 2020, pp. 2446–2454. [4, 13](#)

[39] C. Ni, G. Zhao, X. Wang, Z. Zhu, W. Qin, G. Huang, C. Liu, Y. Chen, Y. Wang, X. Zhang *et al.*, "Recondreamer: Crafting world models for driving scene reconstruction via online restoration," *arXiv preprint arXiv:2411.19548*, 2024. [3, 4](#)

[40] X. Wang, Z. Zhu, G. Huang, B. Wang, X. Chen, and J. Lu, "World-dreamer: Towards general world models for video generation via predicting masked tokens," *arXiv preprint arXiv:2401.09985*, 2024. [3, 4](#)

[41] D. Gao, S. Cai, H. Zhou, H. Wang, I. Soltani, and J. Zhang, "Cardreamer: Open-source learning platform for world model based autonomous driving," *IEEE Internet Things J.*, 2024. [4, 7](#)

[42] A. Dosovitskiy, G. Ros, F. Codevilla, A. Lopez, and V. Koltun, "Carla: An open urban driving simulator," in *Conf. Robot Learn. PMLR*, 2017, pp. 1–16. [4, 6, 7](#)

[43] K. Yang, E. Ma, J. Peng, Q. Guo, D. Lin, and K. Yu, "Bevcontrol: Accurately controlling street-view elements with multi-perspective consistency via bev sketch layout," *arXiv preprint arXiv:2308.01661*, 2023. [3, 4, 5, 12](#)

[44] Y. Wang, J. He, L. Fan, H. Li, Y. Chen, and Z. Zhang, "Driving into the future: Multiview visual forecasting and planning with world model for autonomous driving," in *Proc. IEEE Conf. Comput. Vis. Pattern Recognit.*, 2024, pp. 14749–14759. [3, 4](#)

[45] X. Li, C. Wu, Z. Yang, Z. Xu, D. Liang, Y. Zhang, J. Wan, and J. Wang, "Diverse: Navigation world model for driving simulation via multimodal trajectory prompting and motion alignment," *arXiv preprint arXiv:2504.18576*, 2025. [4](#)

[46] S. Gao, J. Yang, L. Chen, K. Chitta, Y. Qiu, A. Geiger, J. Zhang, and H. Li, "Vista: A generalizable driving world model with high fidelity and versatile controllability," in *Proc. Adv. Neural Inf. Process. Syst.*, 2024. [3, 4, 9, 10, 11, 12](#)

[47] Y. Zhou, M. Simon, Z. M. Peng, S. Mo, H. Zhu, M. Guo, and B. Zhou, "Simgen: Simulator-conditioned driving scene generation," in *Proc. Adv. Neural Inf. Process. Syst.*, vol. 37, 2024, pp. 48838–48874. [4, 12, 13](#)

[48] E. Ma, L. Zhou, T. Tang, Z. Zhang, D. Han, J. Jiang, K. Zhan, P. Jia, X. Lang, H. Sun *et al.*, "Unleashing generalization of end-to-end autonomous driving with controllable long video generation," *arXiv preprint arXiv:2406.01349*, 2024. [4](#)

[49] A. Dosovitskiy, G. Ros, F. Codevilla, A. Lopez, and V. Koltun, "CARLA: An open urban driving simulator," in *Proc. 1st Annu. Conf. Robot Learn.*, 2017, pp. 1–16. [4, 10](#)

[50] Z. Yang, X. Guo, C. Ding, C. Wang, and W. Wu, "Physical informed driving world model," *arXiv preprint arXiv:2412.08410*, 2024. [4, 15](#)

[51] A. Garg and K. M. Krishna, "Imagine-2-drive: High-fidelity world modeling in carla for autonomous vehicles," *arXiv preprint arXiv:2411.10171*, 2024. [4](#)

[52] J. Ni, Y. Guo, Y. Liu, R. Chen, L. Lu, and Z. Wu, "Maskgwm: A generalizable driving world model with video mask reconstruction," *arXiv preprint arXiv:2502.11663*, 2025. [4](#)

[53] J. Yang, S. Gao, Y. Qiu, L. Chen, T. Li, B. Dai, K. Chitta, P. Wu, J. Zeng, P. Luo *et al.*, "Generalized predictive model for autonomous driving," in *Proc. IEEE Conf. Comput. Vis. Pattern Recognit.*, 2024, pp. 14662–14672. [4, 7](#)

[54] J. Zhu, Z. Jia, T. Gao, J. Deng, S. Li, F. Liu, P. Jia, X. Lang, and X. Sun, "Other vehicle trajectories are also needed: A driving world model unifies ego-other vehicle trajectories in video latent space," *arXiv preprint arXiv:2503.09215*, 2025. [4](#)

[55] D. Liang, D. Zhang, X. Zhou, S. Tu, T. Feng, X. Li, Y. Zhang, M. Du, X. Tan, and X. Bai, "Seeing the future, perceiving the future: A unified driving world model for future generation and perception," *arXiv preprint arXiv:2503.13587*, 2025. [4](#)

[56] J. Jiang, G. Hong, M. Zhang, H. Hu, K. Zhan, R. Shao, and L. Nie, "Dive: Efficient multi-view driving scenes generation based on video diffusion transformer," *arXiv preprint arXiv:2504.19614*, 2025. [4](#)

[57] Y. Ji, Z. Zhu, Z. Zhu, K. Xiong, M. Lu, Z. Li, L. Zhou, H. Sun, B. Wang, and T. Lu, "Cogen: 3d consistent video generation via adaptive conditioning for autonomous driving," *arXiv preprint arXiv:2503.22231*, 2025. [4, 12](#)

[58] L. Russell, A. Hu, L. Bertoni, G. Fedoseev, J. Shotton, E. Arani, and G. Corrado, "Gaia-2: A controllable multi-view generative world model for autonomous driving," *arXiv preprint arXiv:2503.20523*, 2025. [4, 11, 12](#)

[59] H. Wang, D. Liu, H. Xie, H. Liu, E. Ma, K. Yu, L. Wang, and B. Wang, "Mila: Multi-view intensive-fidelity long-term video generation world model for autonomous driving," *arXiv preprint arXiv:2503.15875*, 2025. [4, 12](#)

[60] J. Guo, Y. Ding, X. Chen, S. Chen, B. Li, Y. Zou, X. Lyu, F. Tan, X. Qi, Z. Li *et al.*, "Dist-4d: Disentangled spatiotemporal diffusion with metric depth for 4d driving scene generation," *arXiv preprint arXiv:2503.15208*, 2025. [4, 13](#)

[61] Z. Wu, J. Ni, X. Wang, Y. Guo, R. Chen, L. Lu, J. Dai, and Y. Xiong, "Holodrive: Holistic 2d-3d multi-modal street scene generation for autonomous driving," *arXiv preprint arXiv:2412.01407*, 2024. [4](#)

[62] A. Swerdfog, R. Xu, and B. Zhou, "Street-view image generation from a bird's-eye view layout," *IEEE Robot. Autom. Lett.*, 2024. [4](#)

[63] B. Wilson, W. Qi, T. Agarwal, J. Lambert, J. Singh, S. Khandelwal, B. Pan, R. Kumar, A. Hartnett, J. K. Pontes *et al.*, "Argoverse 2: Next generation datasets for self-driving perception and forecasting," *arXiv preprint arXiv:2301.00493*, 2023. [4](#)

[64] X. Hu, W. Yin, M. Jia, J. Deng, X. Guo, Q. Zhang, X. Long, and P. Tan, "Drivingworld: Constructing world model for autonomous driving via video gpt," *arXiv preprint arXiv:2412.19505*, 2024. [4, 12](#)

[65] H. Caesar, J. Kabzan, K. S. Tan, W. K. Fong, E. Wolff, A. Lang, L. Fletcher, O. Beijbom, and S. Omari, "nuplan: A closed-loop ml-based planning benchmark for autonomous vehicles," *arXiv preprint arXiv:2106.11810*, 2021. [4, 7](#)

[66] S. Sreeram, T.-H. Wang, A. Maalouf, G. Rosman, S. Karaman, and D. Rus, "Probing multimodal llms as world models for driving," *arXiv preprint arXiv:2405.05956*, 2024. [4, 7, 8](#)

[67] Z. Huang, J. Zhang, and E. Ohn-Bar, "Neural volumetric world models for autonomous driving," in *Proc. Eur. Conf. Comput. Vis.* Springer, 2025, pp. 195–213. [4](#)

[68] E. Karypidis, I. Kakogeorgiou, S. Gidaris, and N. Komodakis, "Advancing semantic future prediction through multimodal visual sequence transformers," *arXiv preprint arXiv:2501.08303*, 2025. [4](#)

[69] M. Cordts, M. Omran, S. Ramos, T. Rehfeld, M. Enzweiler, R. Benenson, U. Franke, S. Roth, and B. Schiele, "The cityscapes dataset for semantic urban scene understanding," in *Proc. IEEE Conf. Comput. Vis. Pattern Recognit.*, 2016, pp. 3213–3223. [4](#)

[70] A. K. Akan and F. Güney, "Stretchbev: Stretching future instance prediction spatially and temporally," in *Proc. Eur. Conf. Comput. Vis.* Springer, 2022, pp. 444–460. [4, 5](#)

[71] P. Li, S. Ding, X. Chen, N. Hanselmann, M. Cordts, and J. Gall, "Powerbev: a powerful yet lightweight framework for instance prediction in bird's-eye view," *arXiv preprint arXiv:2306.10761*, 2023. [4, 5](#)

[72] S. Hamdan and F. Güney, "Carformer: Self-driving with learned object-centric representations," in *Proc. Eur. Conf. Comput. Vis.* Springer, 2025, pp. 177–193. [4, 5](#)

[73] K. Chitta, A. Prakash, B. Jaeger, Z. Yu, K. Renz, and A. Geiger, "Transfuser: Imitation with transformer-based sensor fusion for autonomous driving," *IEEE Trans. Pattern Anal. Mach. Intell.*, vol. 45, no. 11, pp. 12878–12895, 2022. [4](#)

[74] D. Hafner, T. Lillicrap, J. Ba, and M. Norouzi, "Dream to control: Learning behaviors by latent imagination," in *Proc. Int. Conf. Learn. Represent.*, 2020. [3](#)

[75] D. Hafner, T. P. Lillicrap, M. Norouzi, and J. Ba, "Mastering atari with discrete world models," in *Proc. Int. Conf. Learn. Represent.*, 2021. [3](#)

[76] D. Hafner, J. Pasukonis, J. Ba, and T. Lillicrap, "Mastering diverse domains through world models," *arXiv preprint arXiv:2301.04104*, 2023. [3](#)

[77] X. Li, R. Song, Q. Xie, Y. Wu, N. Zeng, and Y. Ai, "Simworld: A unified benchmark for simulator-conditioned scene generation via world model," *arXiv preprint arXiv:2503.13952*, 2025. [4](#)

[78] T. Feng, W. Wang, X. Wang, Y. Yang, and Q. Zheng, "Clustering based point cloud representation learning for 3d analysis," in *Proc. IEEE Int. Conf. Comput. Vis.*, 2023, pp. 8283–8294. [5](#)

[79] X. Liu, M. Gong, Q. Fang, H. Xie, Y. Li, H. Zhao, and C. Feng, "Lidar-based 4d occupancy completion and forecasting," in *Proc. IEEE/RSJ Int. Conf. Intell. Robot. Syst.* IEEE, 2024, pp. 11102–11109. [5, 6](#)

[80] J. Ma, X. Chen, J. Huang, J. Xu, Z. Luo, J. Xu, W. Gu, R. Ai, and H. Wang, "Cam4docc: Benchmark for camera-only 4d occupancy

forecasting in autonomous driving applications," in *Proc. IEEE Conf. Comput. Vis. Pattern Recognit.*, 2024, pp. 21 486–21 495. [5, 6](#)

[81] X. Wang, Z. Zhu, W. Xu, Y. Zhang, Y. Wei, X. Chi, Y. Ye, D. Du, J. Lu, and X. Wang, "Openoccupancy: A large scale benchmark for surrounding semantic occupancy perception," in *Proc. IEEE Int. Conf. Comput. Vis.*, 2023. [6](#)

[82] X. Li, P. Li, Y. Zheng, W. Sun, Y. Wang, and Y. Chen, "Semi-supervised vision-centric 3d occupancy world model for autonomous driving," in *Proc. Int. Conf. Learn. Represent.*, 2025. [5, 6, 10, 11](#)

[83] X. Tian, T. Jiang, L. Yun, Y. Mao, H. Yang, Y. Wang, Y. Wang, and H. Zhao, "Occ3d: A large-scale 3d occupancy prediction benchmark for autonomous driving," in *Proc. Adv. Neural Inf. Process. Syst.*, vol. 36, 2024. [5, 6, 7, 13, 14](#)

[84] D. Bogdolla, Y. Yang, and J. M. Zöllner, "Muvo: A multimodal generative world model for autonomous driving with geometric representations," in *Proc. IEEE Intell. Veh. Symp.*, 2023. [5, 6, 9, 10](#)

[85] W. Zheng, W. Chen, Y. Huang, B. Zhang, Y. Duan, and J. Lu, "OcwORLD: Learning a 3d occupancy world model for autonomous driving," in *Proc. Eur. Conf. Comput. Vis.* Springer, 2025, pp. 55–72. [5, 6, 9, 10, 11, 12, 14](#)

[86] H. Zhang, Y. Xue, X. Yan, J. Zhang, W. Qiu, D. Bai, B. Liu, S. Cui, and Z. Li, "An efficient occupancy world model via decoupled dynamic flow and image-assisted training," *arXiv preprint arXiv:2412.13772*, 2024. [5, 6, 13, 14](#)

[87] O. Contributors, "Openscene: The largest up-to-date 3d occupancy prediction benchmark in autonomous driving," 2023. [6](#)

[88] Y. Yang, J. Mei, Y. Ma, S. Du, W. Chen, Y. Qian, Y. Feng, and Y. Liu, "Driving in the occupancy world: Vision-centric 4d occupancy forecasting and planning via world models for autonomous driving," in *AAAI Conf. Artif. Intell.*, 2025, pp. 9327–9335. [5, 6, 7, 8, 9, 11, 12, 14](#)

[89] J. Wei, S. Yuan, P. Li, Q. Hu, Z. Gan, and W. Ding, "Occllama: An occupancy-language-action generative world model for autonomous driving," *arXiv preprint arXiv:2409.03272*, 2024. [5, 6, 9, 10, 14](#)

[90] S. Zuo, W. Zheng, Y. Huang, J. Zhou, and J. Lu, "Gaussianworld: Gaussian world model for streaming 3d occupancy prediction," in *Proc. IEEE Conf. Comput. Vis. Pattern Recognit.*, 2025. [5, 6, 12](#)

[91] Z. Yan, W. Dong, Y. Shao, Y. Lu, L. Haiyang, J. Liu, H. Wang, Z. Wang, Y. Wang, F. Remondino *et al.*, "Renderworld: World model with self-supervised 3d label," in *Proc. IEEE Int. Conf. Robot. Autom.*, 2025. [5, 6, 10, 14](#)

[92] J. Chen, H. Xu, Y. Wang, and L.-P. Chau, "Occprophet: Pushing efficiency frontier of camera-only 4d occupancy forecasting with observer-forecaster-refiner framework," in *Proc. Int. Conf. Learn. Represent.*, 2025. [5, 6](#)

[93] T. Xu, H. Lu, X. Yan, Y. Cai, B. Liu, and Y. Chen, "Occ-llm: Enhancing autonomous driving with occupancy-based large language models," in *Proc. IEEE Int. Conf. Robot. Autom.*, 2025. [5, 6](#)

[94] H. Xu, P. Peng, G. Tan, Y. Chang, Y. Zhao, and Y. Tian, "Temporal triplane transformers as occupancy world models," *arXiv preprint arXiv:2503.07338*, 2025. [5, 6](#)

[95] S. Gu, W. Yin, B. Jin, X. Guo, J. Wang, H. Li, Q. Zhang, and X. Long, "Dome: Taming diffusion model into high-fidelity controllable occupancy world model," *arXiv preprint arXiv:2410.10429*, 2024. [5, 6, 13, 14](#)

[96] B. Li, J. Guo, H. Liu, Y. Zou, Y. Ding, X. Chen, H. Zhu, F. Tan, C. Zhang, T. Wang *et al.*, "Uniscene: Unified occupancy-centric driving scene generation," *arXiv preprint arXiv:2412.05435*, 2024. [5, 6](#)

[97] J. Wilson, J. Song, Y. Fu, A. Zhang, A. Capodieci, P. Jayakumar, K. Barton, and M. Ghaffari, "Motionsc: Data set and network for real-time semantic mapping in dynamic environments," *IEEE Robot. Autom. Lett.*, vol. 7, no. 3, pp. 8439–8446, 2022. [6, 13](#)

[98] B. Mersch, X. Chen, J. Behley, and C. Stachniss, "Self-supervised point cloud prediction using 3d spatio-temporal convolutional networks," in *Conf. Robot Learn.* PMLR, 2022, pp. 1444–1454. [6](#)

[99] A. Geiger, P. Lenz, and R. Urtasun, "Are we ready for autonomous driving? the kitti vision benchmark suite," in *Proc. IEEE Conf. Comput. Vis. Pattern Recognit.* IEEE, 2012, pp. 3354–3361. [6](#)

[100] T. Khurana, P. Hu, D. Held, and D. Ramanan, "Point cloud forecasting as a proxy for 4d occupancy forecasting," in *Proc. IEEE Conf. Comput. Vis. Pattern Recognit.*, 2023, pp. 1116–1124. [6](#)

[101] Z. Luo, J. Ma, Z. Zhou, and G. Xiong, "Pcpnet: An efficient and semantic-enhanced transformer network for point cloud prediction," *IEEE Robot. Autom. Lett.*, vol. 8, no. 7, pp. 4267–4274, 2023. [6](#)

[102] X. Zhou, D. Liang, S. Tu, X. Chen, Y. Ding, D. Zhang, F. Tan, H. Zhao, and X. Bai, "Hermes: A unified self-driving world model for simultaneous 3d scene understanding and generation," *arXiv preprint arXiv:2501.14729*, 2025. [6](#)

[103] V. Zyrianov, X. Zhu, and S. Wang, "Learning to generate realistic lidar point clouds," in *Proc. Eur. Conf. Comput. Vis.* Springer, 2022, pp. 17–35. [6, 11](#)

[104] Y. Liao, J. Xie, and A. Geiger, "Kitti-360: A novel dataset and benchmarks for urban scene understanding in 2d and 3d," *IEEE Trans. Pattern Anal. Mach. Intell.*, vol. 45, no. 3, pp. 3292–3310, 2022. [6](#)

[105] L. Zhang, Y. Xiong, Z. Yang, S. Casas, R. Hu, and R. Urtasun, "Copilot4d: Learning unsupervised world models for autonomous driving via discrete diffusion," in *Proc. Int. Conf. Learn. Represent.*, 2024. [6](#)

[106] Q. Hu, Z. Zhang, and W. Hu, "Rangeldlm: Fast realistic lidar point cloud generation," *arXiv preprint arXiv:2403.10094*, 2024. [6, 11](#)

[107] L. Caccia, H. Van Hoof, A. Courville, and J. Pineau, "Deep generative modeling of lidar data," in *Proc. IEEE/RSJ Int. Conf. Intell. Robot. Syst.* IEEE, 2019, pp. 5034–5040. [6](#)

[108] Y. Xiong, W.-C. Ma, J. Wang, and R. Urtasun, "Learning compact representations for lidar completion and generation," in *Proc. IEEE Conf. Comput. Vis. Pattern Recognit.*, 2023, pp. 1074–1083. [6](#)

[109] X. Weng, J. Wang, S. Levine, K. Kitani, and N. Rhinehart, "Inverting the pose forecasting pipeline with spf2: Sequential pointcloud forecasting for sequential pose forecasting," in *Conf. Robot Learn. PMLR*, 2021, pp. 11–20. [6](#)

[110] X. Weng, J. Nan, K.-H. Lee, R. McAllister, A. Gaidon, N. Rhinehart, and K. M. Kitani, "S2net: Stochastic sequential pointcloud forecasting," in *Proc. Eur. Conf. Comput. Vis.* Springer, 2022, pp. 549–564. [6](#)

[111] S. Huang, Z. Gojcic, Z. Wang, F. Williams, Y. Kasten, S. Fidler, K. Schindler, and O. Litany, "Neural lidar fields for novel view synthesis," in *Proc. IEEE Int. Conf. Comput. Vis.*, 2023, pp. 18236–18246. [6](#)

[112] J. Zhang, F. Zhang, S. Kuang, and L. Zhang, "Nerf-lidar: Generating realistic lidar point clouds with neural radiance fields," in *AAAI Conf. Artif. Intell.*, vol. 38, no. 7, 2024, pp. 7178–7186. [6](#)

[113] R. Mahjourian, J. Kim, Y. Chai, M. Tan, B. Sapp, and D. Anguelov, "Occupancy flow fields for motion forecasting in autonomous driving," *IEEE Robot. Autom. Lett.*, vol. 7, no. 2, pp. 5639–5646, 2022. [5](#)

[114] M. Schreiber, S. Hoermann, and K. Dietmayer, "Long-term occupancy grid prediction using recurrent neural networks," in *Proc. IEEE Int. Conf. Robot. Autom.* IEEE, 2019, pp. 9299–9305. [5](#)

[115] A. Sadat, S. Casas, M. Ren, X. Wu, P. Dhawan, and R. Urtasun, "Perceive, predict, and plan: Safe motion planning through interpretable semantic representations," in *Proc. Eur. Conf. Comput. Vis.* Springer, 2020, pp. 414–430. [5, 7, 8](#)

[116] M. Toyungyernsub, E. Yel, J. Li, and M. J. Kochenderfer, "Dynamics-aware spatiotemporal occupancy prediction in urban environments," in *Proc. IEEE/RSJ Int. Conf. Intell. Robot. Syst.* IEEE, 2022, pp. 10 836–10 841. [5](#)

[117] T. Khurana, P. Hu, A. Dave, J. Ziglar, D. Held, and D. Ramanan, "Differentiable raycasting for self-supervised occupancy forecasting," in *Proc. Eur. Conf. Comput. Vis.* Springer, 2022, pp. 353–369. [5, 10, 14](#)

[118] A. E. Sallab, I. Sobh, M. Zahran, and N. Essam, "Lidar sensor modeling and data augmentation with gans for autonomous driving," *arXiv preprint arXiv:1905.07290*, 2019. [6](#)

[119] A. B. Vasudevan, N. Peri, J. Schneider, and D. Ramanan, "Planning with adaptive world models for autonomous driving," *arXiv preprint arXiv:2406.10714*, 2024. [7](#)

[120] C. Diehl, T. S. Sievernich, M. Krüger, F. Hoffmann, and T. Bertram, "Uncertainty-aware model-based offline reinforcement learning for automated driving," *IEEE Robot. Autom. Lett.*, vol. 8, no. 2, pp. 1167–1174, 2023. [7](#)

[121] M. Henaff, A. Canziani, and Y. LeCun, "Model-predictive policy learning with uncertainty regularization for driving in dense traffic," in *Proc. Int. Conf. Learn. Represent.*, 2018. [7](#)

[122] CARLA Team, "CARLA: Autonomous driving leaderboard," <https://leaderboard.carla.org/>, 2022. [7](#)

[123] H. Wang, X. Ye, F. Tao, C. Pan, A. Mallik, B. Yaman, L. Ren, and J. Zhang, "Adawm: Adaptive world model based planning for autonomous driving," in *Proc. Int. Conf. Learn. Represent.*, 2025. 7

[124] A. Nachkov, D. P. Paudel, J.-N. Zaech, D. Scaramuzza, and L. Van Gool, "Dream to drive: Model-based vehicle control using analytic world models," *arXiv preprint arXiv:2502.10012*, 2025. 7

[125] S. Ettlinger, S. Cheng, B. Caine, C. Liu, H. Zhao, S. Pradhan, Y. Chai, B. Sapp, C. R. Qi, Y. Zhou *et al.*, "Large scale interactive motion forecasting for autonomous driving: The waymo open motion dataset," in *Proc. IEEE Int. Conf. Comput. Vis.*, 2021, pp. 9710–9719. 7

[126] Q. Li, X. Jia, S. Wang, and J. Yan, "Think2drive: Efficient reinforcement learning by thinking with latent world model for autonomous driving (in carla-v2)," in *Proc. Eur. Conf. Comput. Vis.* Springer, 2025, pp. 142–158. 7

[127] Y. Chen, Y. Wang, and Z. Zhang, "Drivinggpt: Unifying driving world modeling and planning with multi-modal autoregressive transformers," *arXiv preprint arXiv:2412.18607*, 2024. 7, 13

[128] F. Bartoccioni, E. Ramzi, V. Besnier, S. Venkataraman, T.-H. Vu, Y. Xu, L. Chambon, S. Gidaris, S. Odabas, D. Hurich *et al.*, "Vavim and vavam: Autonomous driving through video generative modeling," *arXiv preprint arXiv:2502.15672*, 2025. 7

[129] Y. Li, Y. Wang, Y. Liu, J. He, L. Fan, and Z. Zhang, "End-to-end driving with online trajectory evaluation via bev world model," *arXiv preprint arXiv:2504.01941*, 2025. 7, 8, 13

[130] P. Li and D. Cui, "Navigation-guided sparse scene representation for end-to-end autonomous driving," in *Proc. Int. Conf. Learn. Represent.*, 2025. 7, 8

[131] W. Zeng, S. Wang, R. Liao, Y. Chen, B. Yang, and R. Urtasun, "Dsdnet: Deep structured self-driving network," in *Proc. Eur. Conf. Comput. Vis.*, 2020. 7, 8

[132] K. Chitta, A. Prakash, and A. Geiger, "Neat: Neural attention fields for end-to-end autonomous driving," in *Proc. IEEE Int. Conf. Comput. Vis.*, 2021, pp. 15793–15803. 7, 8

[133] W. Zeng, W. Luo, S. Suo, A. Sadat, B. Yang, S. Casas, and R. Urtasun, "End-to-end interpretable neural motion planner," in *Proc. IEEE Conf. Comput. Vis. Pattern Recognit.*, 2019, pp. 8660–8669. 7, 8, 14

[134] P. Hu, A. Huang, J. Dolan, D. Held, and D. Ramanan, "Safe local motion planning with self-supervised freespace forecasting," in *Proc. IEEE Conf. Comput. Vis. Pattern Recognit.*, 2021, pp. 12732–12741. 7, 14

[135] N. Karnauchanachari, D. Geromichalos, K. S. Tan, N. Li, C. Erikson, S. Yaghoubi, N. Mehdipour, G. Bernasconi, W. K. Fong, Y. Guo *et al.*, "Towards learning-based planning: The nuplan benchmark for real-world autonomous driving," *arXiv preprint arXiv:2403.04133*, 2024. 7

[136] F. P. Brooks Jr, "The mythical man-month (anniversary ed.)," 1995. 7

[137] B. Paden, M. Čáp, S. Z. Yong, D. Yershov, and E. Frazzoli, "A survey of motion planning and control techniques for self-driving urban vehicles," *IEEE Trans. Intell. Veh.*, vol. 1, no. 1, pp. 33–55, 2016. 7

[138] L. Caltagirone, M. Bellone, L. Svensson, and M. Wahde, "Lidar-based driving path generation using fully convolutional neural networks," in *Proc. IEEE Int. Conf. Intell. Transp. Syst.* IEEE, 2017, pp. 1–6. 7

[139] M. Bojarski, D. Del Testa, D. Dworakowski, B. Firner, B. Flepp, P. Goyal, L. D. Jackel, M. Monfort, U. Muller, J. Zhang *et al.*, "End to end learning for self-driving cars," *arXiv preprint arXiv:1604.07316*, 2016. 7

[140] C. Richter and N. Roy, "Safe visual navigation via deep learning and novelty detection," 2017. 7

[141] C. Vallon, Z. Ercan, A. Carvalho, and F. Borrelli, "A machine learning approach for personalized autonomous lane change initiation and control," in *Proc. IEEE Intell. Veh. Symp.* IEEE, 2017, pp. 1590–1595. 7

[142] Q. Huy, S. Mita, H. T. N. Nejad, and L. Han, "Dynamic and safe path planning based on support vector machine among multi moving obstacles for autonomous vehicles," *IEICE Trans. Inf. Syst.*, vol. 96, no. 2, pp. 314–328, 2013. 7

[143] S. Mozaffari, O. Y. Al-Jarrah, M. Dianati, P. Jennings, and A. Mouzakitis, "Deep learning-based vehicle behavior prediction for autonomous driving applications: A review," *IEEE Trans. Intell. Transp. Syst.*, 2020. 7

[144] S. Lefevre, A. Carvalho, and F. Borrelli, "A learning-based framework for velocity control in autonomous driving," *IEEE Trans. Autom. Sci. Eng.*, vol. 13, no. 1, pp. 32–42, 2015. 7

[145] D. A. Pomerleau, "Alvinn: An autonomous land vehicle in a neural network," CARNEGIE-MELLON UNIV PITTSBURGH PA ARTIFICIAL INTELLIGENCE AND PSYCHOLOGY ..., Tech. Rep., 1989. 7

[146] C. Lu, J. Gong, C. Lv, X. Chen, D. Cao, and Y. Chen, "A personalized behavior learning system for human-like longitudinal speed control of autonomous vehicles," *Sensors*, vol. 19, no. 17, p. 3672, 2019. 7

[147] A. Prakash, K. Chitta, and A. Geiger, "Multi-modal fusion transformer for end-to-end autonomous driving," in *Proc. IEEE Conf. Comput. Vis. Pattern Recognit.*, 2021. 7

[148] X. Jia, L. Chen, P. Wu, J. Zeng, J. Yan, H. Li, and Y. Qiao, "Towards capturing the temporal dynamics for trajectory prediction: a coarse-to-fine approach," in *Conf. Robot Learn. PMLR*, 2023, pp. 910–920. 7

[149] X. Jia, L. Sun, M. Tomizuka, and W. Zhan, "Ide-net: Interactive driving event and pattern extraction from human data," *IEEE Robot. Autom. Lett.*, vol. 6, no. 2, pp. 3065–3072, 2021. 7

[150] X. Jia, P. Wu, L. Chen, Y. Liu, H. Li, and J. Yan, "Hdgt: Heterogeneous driving graph transformer for multi-agent trajectory prediction via scene encoding," *IEEE Trans. Pattern Anal. Mach. Intell.*, 2023. 7

[151] F. Codevilla, E. Santana, A. M. López, and A. Gaidon, "Exploring the limitations of behavior cloning for autonomous driving," in *Proc. IEEE Int. Conf. Comput. Vis.*, 2019, pp. 9329–9338. 7

[152] H. Lu, X. Jia, Y. Xie, W. Liao, X. Yang, and J. Yan, "Activead: Planning-oriented active learning for end-to-end autonomous driving," *arXiv preprint arXiv:2403.02877*, 2024. 7

[153] T. Phan-Minh, E. C. Grigore, F. A. Boulton, O. Beijbom, and E. M. Wolff, "Covernet: Multimodal behavior prediction using trajectory sets," in *Proc. IEEE Conf. Comput. Vis. Pattern Recognit.*, 2020, pp. 14074–14083. 8

[154] M. Treiber, A. Hennecke, and D. Helbing, "Congested traffic states in empirical observations and microscopic simulations," *Phys. Rev. E*, vol. 62, no. 2, p. 1805, 2000. 8, 9

[155] D. Dauner, M. Hallgarten, A. Geiger, and K. Chitta, "Parting with misconceptions about learning-based vehicle motion planning," in *Conf. Robot Learn.*, 2023. 8, 9

[156] S. LaValle, "Rapidly-exploring random trees: A new tool for path planning," *Research Report 9811*, 1998. 8, 9

[157] J. J. Kuffner and S. M. LaValle, "Rrt-connect: An efficient approach to single-query path planning," in *Proc. IEEE Int. Conf. Robot. Autom.*, vol. 2. IEEE, 2000, pp. 995–1001. 8, 9

[158] S. Karaman and E. Frazzoli, "Incremental sampling-based algorithms for optimal motion planning," *Robot. Sci. Syst. VI*, vol. 104, no. 2, pp. 267–274, 2010. 8, 9

[159] —, "Sampling-based algorithms for optimal motion planning," *Int. J. Robot. Res.*, vol. 30, no. 7, pp. 846–894, 2011. 8, 9

[160] J. Ziegler and C. Stiller, "Spatiotemporal state lattices for fast trajectory planning in dynamic on-road driving scenarios," in *Proc. IEEE/RSJ Int. Conf. Intell. Robot. Syst.* IEEE, 2009, pp. 1879–1884. 8, 9

[161] M. McNaughton, C. Urmson, J. M. Dolan, and J.-W. Lee, "Motion planning for autonomous driving with a conformal spatiotemporal lattice," in *Proc. IEEE Int. Conf. Robot. Autom.* IEEE, 2011, pp. 4889–4895. 8, 9

[162] M. Werling, S. Kammer, J. Ziegler, and L. Gröll, "Optimal trajectories for time-critical street scenarios using discretized terminal manifolds," *Int. J. Robot. Res.*, vol. 31, no. 3, pp. 346–359, 2012. 8, 9

[163] H. Fan, F. Zhu, C. Liu, L. Zhang, L. Zhuang, D. Li, W. Zhu, J. Hu, H. Li, and Q. Kong, "Baidu apollo em motion planner," *arXiv preprint arXiv:1807.08048*, 2018. 8, 9

[164] J. P. Rastelli, R. Lattarulo, and F. Nashashibi, "Dynamic trajectory generation using continuous-curvature algorithms for door to door assistance vehicles," in *Proc. 2014 IEEE Intell. Veh. Symp.* IEEE, 2014, pp. 510–515. 8, 9

[165] O. Khatib and J. Le Maitre, "Dynamic control of manipulators operating in a complex environment," in *Proc. 3rd CISM-IFTOMM Symp. Theory Pract. Robots Manip.*, vol. 267, 1978. 8, 9

[166] O. Khatib, "Real-time obstacle avoidance for manipulators and mobile robots," in *Autonomous Robot Vehicles*. Springer, 1986, pp. 396–404. 8, 9

[167] J. Ren, K. A. McIsaac, and R. V. Patel, "Modified newton's method applied to potential field-based navigation for mobile robots," *IEEE Trans. Robot.*, vol. 22, no. 2, pp. 384–391, 2006. [8](#) [9](#)

[168] B. Lu, H. He, H. Yu, H. Wang, G. Li, M. Shi, and D. Cao, "Hybrid path planning combining potential field with sigmoid curve for autonomous driving," *Sensors*, vol. 20, no. 24, p. 7197, 2020. [9](#)

[169] F. Bounini, D. Gingras, H. Pollart, and D. Gruyer, "Modified artificial potential field method for online path planning applications," in *Proc. IEEE Intell. Veh. Symp.* IEEE, 2017, pp. 180–185. [9](#)

[170] E. Galceran, R. M. Eustice, and E. Olson, "Toward integrated motion planning and control using potential fields and torque-based steering actuation for autonomous driving," in *Proc. IEEE Intell. Veh. Symp.* IEEE, 2015, pp. 304–309. [9](#)

[171] D. González, J. Pérez, V. Milanés, and F. Nashashibi, "A review of motion planning techniques for automated vehicles," *IEEE Trans. Intell. Transp. Syst.*, vol. 17, no. 4, pp. 1135–1145, 2015. [8](#) [9](#)

[172] C. Zhou, B. Huang, and P. Fränti, "A review of motion planning algorithms for intelligent robots," *J. Intell. Manuf.*, vol. 33, no. 2, pp. 387–424, 2022. [8](#) [9](#)

[173] Y. Kuwata, J. Teo, G. Fiore, S. Karaman, E. Frazzoli, and J. P. How, "Real-time motion planning with applications to autonomous urban driving," *IEEE Trans. Control Syst. Technol.*, vol. 17, no. 5, pp. 1105–1118, 2009. [8](#)

[174] M. Buehler, K. Iagnemma, and S. Singh, *The DARPA Urban Challenge: Autonomous Vehicles in City Traffic*, 1st ed. Springer Publishing Company, Incorporated, 2009. [8](#)

[175] A. Pongpunwattana and R. Rysdyk, "Real-time planning for multiple autonomous vehicles in dynamic uncertain environments," *J. Aerosp. Comput. Inf. Commun.*, vol. 1, no. 12, pp. 580–604, 2004. [8](#)

[176] X. Li, Z. Sun, D. Cao, Z. He, and Q. Zhu, "Real-time trajectory planning for autonomous urban driving: Framework, algorithms, and verifications," *IEEE/ASME Trans. Mechatronics*, vol. 21, no. 2, pp. 740–753, 2015. [8](#)

[177] K. Chu, M. Lee, and M. Sunwoo, "Local path planning for off-road autonomous driving with avoidance of static obstacles," *Proc. IEEE Int. Conf. Intell. Transp. Syst.*, vol. 13, no. 4, pp. 1599–1616, 2012. [8](#)

[178] M. Montemerlo, J. Becker, S. Bhat, H. Dahlkamp, D. Dolgov, S. Etinger, D. Haehnel, T. Hilden, G. Hoffmann, B. Huhnke, D. Johnston, S. Klumpp, D. Langer, A. Levandowski, J. Levinson, J. Marcil, D. Orenstein, J. Paefgen, I. Penny, A. Petrovskaya, M. Pflueger, G. Stanek, D. Stavens, A. Vogt, and S. Thrun, "Junior: The stanford entry in the urban challenge," *J. Field Robot.*, vol. 25, no. 9, p. 569–597, sep 2008. [8](#)

[179] T. Gu, J. M. Dolan, and J.-W. Lee, "Runtime-bounded tunable motion planning for autonomous driving," in *Proc. IEEE Intell. Veh. Symp.* IEEE, 2016, pp. 1301–1306. [9](#)

[180] J. Bohren, T. Foote, J. Keller, A. Kushleyev, D. Lee, A. Stewart, P. Vernaza, J. Derenick, J. Spletzer, and B. Satterfield, "Little ben: The ben franklin racing team's entry in the 2007 darpa urban challenge," in *The DARPA Urban Challenge*. Springer, 2009, pp. 231–255. [9](#)

[181] S. Kammel, J. Ziegler, B. Pitzer, M. Werling, T. Gindele, D. Jagzent, J. Schöder, M. Thuy, M. Goebel, F. von Hundelshausen *et al.*, "Team anneway's autonomous system for the darpa urban challenge 2007," in *The DARPA Urban Challenge*. Springer, 2009, pp. 359–391. [9](#)

[182] Z. Boroujeni, D. Goehring, F. Ulbrich, D. Neumann, and R. Rojas, "Flexible unit a-star trajectory planning for autonomous vehicles on structured road maps," in *Proc. IEEE Int. Conf. Veh. Electron. Saf.* IEEE, 2017, pp. 7–12. [9](#)

[183] D. Dolgov, S. Thrun, M. Montemerlo, and J. Diebel, "Practical search techniques in path planning for autonomous driving," *Ann Arbor*, vol. 1001, no. 48105, pp. 18–80, 2008. [9](#)

[184] Z. Ajanovic, B. Lacevic, B. Shyrokau, M. Stoltz, and M. Horn, "Search-based optimal motion planning for automated driving," in *Proc. IEEE/RSJ Int. Conf. Intell. Robot. Syst.* IEEE, 2018, pp. 4523–4530. [9](#)

[185] Z. Ajanovic, "Towards superhuman autonomous vehicles," 2019. [9](#)

[186] B. Adabala and Z. Ajanović, "A multi-heuristic search-based motion planning for automated parking," in *Proc. XXIX Int. Conf. Inf. Commun. Automat. Technol.* IEEE, 2023, pp. 1–8. [9](#)

[187] Z. Ajanović, E. Regolin, B. Shyrokau, H. Ćatić, M. Horn, and A. Ferrara, "Search-based task and motion planning for hybrid systems: Agile autonomous vehicles," *arXiv preprint arXiv:2301.10384*, 2023. [9](#)

[188] S. W. Kim, J. Phlion, A. Torralba, and S. Fidler, "Drivegan: Towards a controllable high-quality neural simulation," in *Proc. IEEE Conf. Comput. Vis. Pattern Recognit.*, 2021, pp. 5820–5829. [9](#) [11](#)

[189] R. Gao, K. Chen, E. Xie, L. HONG, Z. Li, D.-Y. Yeung, and Q. Xu, "Magicdrive: Street view generation with diverse 3d geometry control," in *Proc. Int. Conf. Learn. Represent.*, 2024. [9](#)

[190] L. Feng, Q. Li, Z. Peng, S. Tan, and B. Zhou, "Trafficgen: Learning to generate diverse and realistic traffic scenarios," in *ICRA*, 2023. [9](#)

[191] S. Tan, B. Ivanovic, X. Weng, M. Pavone, and P. Krahenbuehl, "Language conditioned traffic generation," in *Conf. Robot Learn.*, 2023. [9](#) [13](#)

[192] W. Ding, Y. Cao, D. Zhao, C. Xiao, and M. Pavone, "Realgen: Retrieval augmented generation for controllable traffic scenarios," in *Proc. Eur. Conf. Comput. Vis.* Springer, 2024, pp. 93–110. [9](#)

[193] D. Dauner, M. Hallgarten, T. Li, X. Weng, Z. Huang, Z. Yang, H. Li, I. Gilitschenski, B. Ivanovic, M. Pavone *et al.*, "Navsim: Data-driven non-reactive autonomous vehicle simulation and benchmarking," in *Proc. Adv. Neural Inf. Process. Syst.*, vol. 37, 2024, pp. 28706–28719. [9](#)

[194] J. Zhao, J. Zhuang, Q. Zhou, T. Ban, Z. Xu, H. Zhou, J. Wang, G. Wang, Z. Li, and B. Li, "Kigras: Kinematic-driven generative model for realistic agent simulation," *IEEE Robot. Autom. Lett.*, 2024. [9](#)

[195] W. Wu, X. Feng, Z. Gao, and Y. Kan, "Smart: Scalable multi-agent real-time motion generation via next-token prediction," in *Proc. Adv. Neural Inf. Process. Syst.*, vol. 37, 2024, pp. 114048–114071. [9](#)

[196] W. Zheng, Z. Xia, Y. Huang, S. Zuo, J. Zhou, and J. Lu, "Doe-1: Closed-loop autonomous driving with large world model," *arXiv preprint arXiv:2412.09627*, 2024. [9](#) [13](#)

[197] S. Suo, S. Regalado, S. Casas, and R. Urtasun, "Trafficsim: Learning to simulate realistic multi-agent behaviors," in *Proc. IEEE Conf. Comput. Vis. Pattern Recognit.*, 2021, pp. 10400–10409. [9](#) [12](#)

[198] Z. Zhang, A. Liniger, D. Dai, F. Yu, and L. Van Gool, "Trafficbots: Towards world models for autonomous driving simulation and motion prediction," in *Proc. IEEE Int. Conf. Robot. Autom.* IEEE, 2023, pp. 1522–1529. [9](#) [12](#)

[199] K. Chen, W. Sun, H. Cheng, and S. Zheng, "Rift: Closed-loop rl fine-tuning for realistic and controllable traffic simulation," *arXiv preprint arXiv:2505.03344*, 2025. [9](#)

[200] D. Krajzewicz, J. Erdmann, M. Behrisch, and L. Bieker, "Recent development and applications of sumo-simulation of urban mobility," *International journal on advances in systems and measurements*, vol. 5, no. 3&4, 2012. [10](#)

[201] C. Gulino, J. Fu, W. Luo, G. Tucker, E. Bronstein, Y. Lu, J. Harb, X. Pan, Y. Wang, X. Chen *et al.*, "Waymax: An accelerated, data-driven simulator for large-scale autonomous driving research," in *Proc. Adv. Neural Inf. Process. Syst.*, vol. 36, 2024. [10](#)

[202] Q. Li, Z. Peng, L. Feng, Q. Zhang, Z. Xue, and B. Zhou, "Metadrive: Composing diverse driving scenarios for generalizable reinforcement learning," *IEEE Trans. Pattern Anal. Mach. Intell.*, vol. 45, no. 3, pp. 3461–3475, 2022. [10](#)

[203] Z. Yang, Y. Chen, J. Wang, S. Manivasagam, W.-C. Ma, A. J. Yang, and R. Urtasun, "Unisim: A neural closed-loop sensor simulator," in *Proc. IEEE Conf. Comput. Vis. Pattern Recognit.*, 2023, pp. 1389–1399. [10](#) [13](#)

[204] G. Yan, J. Pi, J. Guo, Z. Luo, M. Dou, N. Deng, Q. Huang, D. Fu, L. Wen, P. Cai *et al.*, "Oasim: an open and adaptive simulator based on neural rendering for autonomous driving," *arXiv preprint arXiv:2402.03830*, 2024. [10](#)

[205] Z. Huang, Z. Sheng, Z. Wan, Y. Qu, Y. Luo, B. Wang, P. Li, Y.-J. Chen, J. Chen, K. Long *et al.*, "Sky-drive: A distributed multi-agent simulation platform for socially-aware and human-ai collaborative future transportation," *arXiv preprint arXiv:2504.18010*, 2025. [10](#)

[206] T. Yan, D. Wu, W. Han, J. Jiang, X. Zhou, K. Zhan, C.-z. Xu, and J. Shen, "Drivingsphere: Building a high-fidelity 4d world for closed-loop simulation," in *Proc. IEEE Conf. Comput. Vis. Pattern Recognit.*, 2025. [10](#) [13](#)

[207] L. Wenl, D. Fu, S. Mao, P. Cai, M. Dou, Y. Li, and Y. Qiao, "Limsim: A long-term interactive multi-scenario traffic simulator," in *Proc. IEEE Int. Conf. Intell. Transp. Syst.* IEEE, 2023, pp. 1255–1262. [10](#)

- [208] D. Fu, W. Lei, L. Wen, P. Cai, S. Mao, M. Dou, B. Shi, and Y. Qiao, "Limsim++: A closed-loop platform for deploying multimodal llms in autonomous driving," in *Proc. IEEE Intell. Veh. Symp. IEEE*, 2024, pp. 1084–1090. 10
- [209] D. Fu, N. Zhong, X. Han, P. Cai, L. Wen, S. Mao, B. Shi, and Y. Qiao, "Limsim series: An autonomous driving simulation platform for validation and enhancement," *arXiv preprint arXiv:2502.09170*, 2025. 10
- [210] M. Pan, J. Liu, R. Zhang, P. Huang, X. Li, L. Liu, and S. Zhang, "Renderocc: Vision-centric 3d occupancy prediction with 2d rendering supervision," in *Proc. IEEE Int. Conf. Robot. Autom.*, 2024. 10
- [211] Y. Huang, W. Zheng, B. Zhang, J. Zhou, and J. Lu, "Selfocc: Self-supervised vision-based 3d occupancy prediction," in *Proc. IEEE Conf. Comput. Vis. Pattern Recognit.*, 2024, pp. 19 946–19 956. 10, 14
- [212] C. Zhang, J. Yan, Y. Wei, J. Li, L. Liu, Y. Tang, Y. Duan, and J. Lu, "Occnerf: Self-supervised multi-camera occupancy prediction with neural radiance fields," *arXiv preprint arXiv:2312.09243*, 2023. 10
- [213] H. Yang, S. Zhang, D. Huang, X. Wu, H. Zhu, T. He, S. Tang, H. Zhao, Q. Qiu, B. Lin *et al.*, "Unipad: A universal pre-training paradigm for autonomous driving," in *Proc. IEEE Conf. Comput. Vis. Pattern Recognit.*, 2024, pp. 15 238–15 250. 10, 11
- [214] L. Zhang, Y. Xiong, Z. Yang, S. Casas, R. Hu, and R. Urtasun, "Learning unsupervised world models for autonomous driving via discrete diffusion," *arXiv preprint arXiv:2311.01017*, 2023. 10
- [215] H. Zhu, Z. Dong, K. Topollai, and A. Choromanska, "Ad-ljepa: Self-supervised spatial world models with joint embedding predictive architecture for autonomous driving with lidar data," *arXiv preprint arXiv:2501.04969*, 2025. 11
- [216] C. Min, D. Zhao, L. Xiao, Y. Nie, and B. Dai, "Uniworld: Autonomous driving pre-training via world models," *arXiv preprint arXiv:2308.07234*, 2023. 11
- [217] Z. Huang, J. Zhang, and E. Ohn-Bar, "Neural volumetric world models for autonomous driving," in *Proc. Eur. Conf. Comput. Vis. Springer*, 2024, pp. 195–213. 11, 12
- [218] C. Min, L. Xiao, D. Zhao, Y. Nie, and B. Dai, "Occupancy-mae: Self-supervised pre-training large-scale lidar point clouds with masked occupancy autoencoders," *IEEE Trans. Intell. Veh.*, 2023. 11
- [219] B. Kerbl, G. Kopanas, T. Leimkühler, and G. Drettakis, "3d gaussian splatting for real-time radiance field rendering," vol. 42, no. 4, pp. 1–14, 2023. 12
- [220] X. Guo, C. Ding, H. Dou, X. Zhang, W. Tang, and W. Wu, "Infinitydrive: Breaking time limits in driving world models," *arXiv preprint arXiv:2412.01522*, 2024. 12
- [221] Y. Zhang, J. Zhang, Z. Wang, J. Xu, and D. Huang, "Vision-based 3d occupancy prediction in autonomous driving: a review and outlook," *arXiv preprint arXiv:2405.02595*, 2024. 13
- [222] Y. Li, L. Fan, J. He, Y. Wang, Y. Chen, Z. Zhang, and T. Tan, "Enhancing end-to-end autonomous driving with latent world model," *arXiv preprint arXiv:2406.08481*, 2024. 13
- [223] A.-Q. Cao and R. De Charette, "Monoscene: Monocular 3d semantic scene completion," in *Proc. IEEE Conf. Comput. Vis. Pattern Recognit.*, 2022. 13
- [224] Y. Huang, W. Zheng, Y. Zhang, J. Zhou, and J. Lu, "Tri-perspective view for vision-based 3d semantic occupancy prediction," in *Proc. IEEE Conf. Comput. Vis. Pattern Recognit.*, 2023, pp. 9223–9232. 14
- [225] Y. Hu, J. Yang, L. Chen, K. Li, C. Sima, X. Zhu, S. Chai, S. Du, T. Lin, W. Wang *et al.*, "Planning-oriented autonomous driving," in *Proc. IEEE Conf. Comput. Vis. Pattern Recognit.*, 2023, pp. 17 853–17 862. 14